FLAVOR ASYMMETRY OF THE SEA QUARK DISTRIBUTIONS

Jen-Chieh Peng and Gerald T. Garvey

September 6, 1999

Physics Division
Los Alamos National Laboratory
Los Alamos, NM 87545 USA

CONTENTS

Abstract

Recent deep inelastic scattering and Drell-Yan experiments have revealed a surprisingly large asymmetry between the up and down sea quark distributions in the nucleon. This result strongly suggests that the mesonic degrees of freedom play an important role in the description of the parton distributions in hadrons. In this article, we review the current status of the flavor asymmetry of the nucleon sea. The implications of the pionic models as well as possible future measurements are also discussed.

1. INTRODUCTION

The first direct evidence for point-like constituents in the nucleons came from the observation of scaling phenomenon in Deep-Inelastic Scattering (DIS) experiments [1, 2] at SLAC. These point-like charged constituents, called partons, were found to be spin-1/2 fermions. These partons were initially identified as the quarks in the Constituent Quark Models (CQM). However, it was soon realized that valence quarks alone could not account for the large enhancement of the cross sections at small Bjorken-x, the fraction of nucleon momentum carried by the partons. These swarm of low-momentum partons, dubbed wee-partons by Feynman [3], was interpreted as the quark and antiquark sea of the nucleon. DIS experiments therefore provided the first evidence for the existence of antiquarks in the nucleon.

The observation of partons in DIS experiments paved the road to the formulation of Quantum Chromodynamics (QCD) as the theory for strong interaction. Nevertheless, the exact form of the parton distribution functions can not be deduced from perturbative QCD. Like many other static properties of hadrons, the parton distribution functions belong to the domain of non-perturbative QCD. In spite of great progress [4] made in Lattice Gauge Theory (LGT) in treating the bound-state properties of hadrons, it remains a challenge to predict the parton distributions using LGT.

Until parton distributions can be readily calculated from first principles, they are best determined from experiments. Electroweak processes such as DIS and lepton-pair production provide the cleanest means to extract information on the parton distributions. There are at least two reasons why it is important to measure the parton distribution functions. First, the description of hard processes in high energy interactions requires parton distribution functions as an essential input. Second, many aspects of the parton distributions, such as sum-rules, scaling-violation, asymptotic behaviors at large and small x, and flavor and spin structures, can be compared with the predictions of perturbative as well as non-perturbative QCD.

In this article, we review the status of our current knowledge on the flavor dependence of the sea quark distributions in hadrons. The recent observation of a striking flavor asymmetry of the nucleon sea has profound implications on the importance of meson degrees of freedom for the description of parton substructures in the nucleon. In Section 2, we review the early studies of the nucleon sea in DIS and lepton-pair production. The crucial recent experiments establishing the up/down flavor asymmetry of the nucleon sea are discussed in Section 3. The various theoretical models for explaining the $\bar{u}/\bar{d}$ asymmetry are described in Section 4. The implications of meson-cloud models on other aspects of the parton structure functions are discussed in Section 5. Finally, we present future prospects in Section 6, followed by conclusion in Section 7.

2. EARLY STUDIES OF THE NUCLEON SEA

2.1 Deep Inelastic Scattering

Although scaling behavior in inelastic electron scattering was predicted by Bjorken [5] based on the framework of current algebra, its confirmation by the SLAC experiments still came as a major surprise. A simple and intuitive picture for explaining the scaling behavior is the parton model advanced by Feynman [3, 6]. In this model, the electron-nucleon deep-inelastic scattering is described as an incoherent sum of elastic electron-parton scattering. However, the nature of the partons within the nucleon was not specified by Feynman. Some authors [7, 8, 9, 10] speculated that the partons are the 'bare nucleon' plus the pion cloud, while others [11, 12, 13] believed they are the quarks introduced by Gell-Mann [14] and Zweig [15]. The latter scenario was strongly supported by the measurement of R, ratio of the longitudinally over transversely polarized photon cross sections, showing the spin-1/2 character of the partons.

Evidence for quark-antiquark sea in the nucleon came from the observation that the structure function $F_2(x)$ approaches a constant value as $x \to 0$ [16]. If the proton is made up of only three quarks, or any finite number of quarks, $F_2(x)$ is expected to vanish as $x \to 0$. Bjorken and Paschos [11] therefore assumed that the nucleon consists of three quarks in a background of an indefinite number of quark-antiquark pairs. Kuti and Weisskopf [12] further included gluons among the constituents of nucleons in order to account for the missing momentum not carried by the quarks and antiquarks alone.

The importance of the quark-antiquark pairs in the nucleon is in sharp contrast to the situation for the atomic system, where particle-antiparticle pairs play a relatively minor role (such as the polarization of the vacuum). In strong interactions, pairs of virtual fermions or virtual Goldstone bosons are readily produced as a result of the relatively large magnitude of the coupling constant α_s, and they form an integral part of the nucleon's structure.

Neutrino-induced DIS experiments allowed the separation of sea quarks from the valence quarks. Recall that

$$\begin{aligned} F_2^{\nu p}(x) &= 2x \sum_i \left[q_i(x) + \bar{q}_i(x)\right], \\ F_3^{\nu p}(x) &= 2 \sum_i \left[q_i(x) - \bar{q}_i(x)\right] = 2 \sum_i q_i^v(x), \end{aligned} \tag{1}$$

where i denotes the flavor of the quarks. Note that the valence quark distribution is defined as the difference of the quark and antiquark distributions, $q_i^v(x) = q_i(x) - \bar{q}_i(x)$. Eq. 1 shows that the valence quark distribution is simply $F_3^{\nu p}(x)/2$, while the sea quark distribution is given by $F_2^{\nu p}(x)/2x - F_3^{\nu p}(x)/2$. The $F_2(x)$ and $F_3(x)$ data from the CDHS experiment [17] clearly showed that the valence quark distributions dominate at $x > 0.2$, while the sea quarks are at small x.

The earliest parton models assumed that the proton sea was flavor symmetric, even though the valence quark distributions are clearly flavor asymmetric. Inherent in this assumption is that the content of the sea is independent of the valence quark's composition. Therefore, the proton and neutron are expected to have identical sea-quark distributions. The flavor symmetry assumption was not based on any known physics, and it remained to be tested by experiments. Neutrino-induced charm production experiments [18, 19], which are sensitive to the $s \to c$ process, provided strong evidences that the strange-quark content in the nucleon is only about half of the up or down sea quarks. Such flavor asymmetry is attributed to the much heavier strange-quark mass compared to the up and down quarks. The similar masses for the up and down quarks suggest that the nucleon sea should be nearly up-down symmetric. A very interesting method to check this assumption is to measure the Gottfried integral in DIS, as discussed next.

2.2 Gottfried Sum Rule

In 1967, Gottfried studied electron-proton scattering assuming that the proton consists of three constituent quarks [20]. He showed that the total electron-proton cross section (elastic plus inelastic) is identical to the Rutherford scattering from a point charge. Gottfried derived a sum rule

$$I_2^p = \int_0^1 F_2^p(x, Q^2)/x \; dx = \sum_i (Q_i^p)^2 = 1, \tag{2}$$

where Q_i^p is the charge of the ith quark in the proton. Gottfried expressed great skepticism that this sum rule would be confirmed by the forthcoming SLAC experiment by stating "I think Prof. Bjorken and I constructed the sum rules in the hope of destroying the quark model" [21]. Indeed, Eq. 2 was not confirmed by the experiments, not because of the failure of the quark model, but because of the presence of quark-antiquark sea. In fact, the infinite number of the sea partons makes I_2^p diverge. A closely related sum rule, now called the Gottfried Sum Rule (GSR), avoids this problem by considering the difference of the proton and neutron cross sections, namely,

$$I_2^p - I_2^n = \int_0^1 [F_2^p(x, Q^2) - F_2^n(x, Q^2)]/x \; dx = \sum_i [(Q_i^p)^2 - (Q_i^n)^2] = 1/3. \tag{3}$$

In deriving Eq. 3, it was assumed that the sea quarks in the proton and neutron are related by charge symmetry (see Section 4.5).

Soon after the discovery of scaling in electron-proton DIS, electron-deuterium scattering experiments were carried out to extract the electron-neutron cross sections. The comparison of $e - p$ with $e - n$ data was very important for distinguishing early competing theoretical models [16]. These data also allowed a first evaluation [22] of the Gottfried integral in 1970. The first result for the Gottfried integral was 0.19, considerably less than 1/3. Note that the data only covered $x > 0.08$, and it was assumed that $F_2^p - F_2^n$ follows Regge behavior (proportional to $x^{1/2}$) in the unmeasured small-x region. Due to the $1/x$ factor in the integrand, the small-x region could have potentially large contributions to the Gottfried integral. Moreover, it was not clear if $F_2^p - F_2^n$ would indeed follow the Regge behavior at small x, and if so, at what value of x. By 1973, new data were available down to $x = 0.05$ and the Gottfried integral was evaluated to be 0.28 [23], considerably larger than the first result. It should be pointed out that these data were taken at relatively low values of Q^2. Furthermore, Q^2 varies as a function of x.

Although the large systematic errors associated with the unmeasured small-x region prevented a sensitive test of the GSR, Field and Feynman [24] nevertheless interpreted the early SLAC data as strong indications that GSR is violated and that the $\bar{u}$ and $\bar{d}$ distributions in the proton are different. The relationship between the Gottfried integral and the $\bar{d}/\bar{u}$ asymmetry is clearly seen in the parton model, namely,

$$\int_0^1 [F_2^p(x,Q^2) - F_2^n(x,Q^2)]/x \; dx = \frac{1}{3} + \frac{2}{3}\int_0^1 [\bar{u}(x) - \bar{d}(x)]dx. \tag{4}$$

Eq. 4 clearly shows that the early SLAC data on GSR implied $\bar{d} > \bar{u}$, at least for certain region of x. Field and Feynman further suggested that Pauli-blocking from the valence quarks would inhibit the $\bar{u}u$ sea more than the $\bar{d}d$ sea, hence creating an asymmetric nucleon sea.

The SLAC DIS experiments were followed by several muon-induced DIS experiments at Fermilab and at CERN. Using high energy muon beams, these experiments reached much larger values of Q^2 and they clearly established [25, 26, 27] the scaling-violation phenomenon in DIS. The Gottfried integral was also evaluated in muon DIS experiments [28, 29]. Figure 1 compares the data from the European Muon Collaboration (EMC) [28] with earlier electron data from SLAC [30]. The coverages in x are similar in these two experiments, even though the Q^2 values covered by the EMC are much larger. Figure 1 shows that $F_2^p - F_2^n$ from EMC tend to shift towards smaller x relative to the SLAC data, in qualitative agreement with the QCD Q^2-evolution. The Gottfried integral determined from the EMC experiment is $0.235 + 0.110 - 0.099$, consistent with that from the SLAC, but still lower than 1/3.

Despite the fact that all measurements of Gottfried integral consistently showed a value lower than 1/3, the large systematic errors prevented a definitive conclusion. As a result, all parametrizations [31, 32, 33, 34, 35] of the parton distributions based on global fits to existing data before 1990 assumed a symmetric $\bar{u}$, $\bar{d}$ sea. As discussed later, compelling evidence for an asymmetric light-quark sea awaited new experimental inputs.

2.3 Drell-Yan Process

The first high-mass dilepton production experiment [36] was carried out at the AGS in 1969, soon after scaling was discovered at SLAC. Drell and Yan [37] interpreted the data within the parton model, in which a quark-antiquark pair annihilate into a virtual photon decaying subsequently into a lepton pair. This simple model was capable of explaining several pertinent features of the data, including the overall magnitude of the cross sections, the scaling behavior of the cross sections, and the polarization of the virtual photons. The high-mass continuum lepton-pair production is therefore called the Drell-Yan (DY) process.

Since the underlying mechanism for the DY process involves the annihilation of a quark with an antiquark, it is not surprising that this process can be used to probe the antiquark contents of the beam or target hadrons. In the parton model, the DY cross section is given by

$$\frac{d^2\sigma}{dM^2 dx_F} = \frac{4\pi\alpha^2}{9M^2 s}\frac{1}{(x_1+x_2)}\sum_a e_a^2[q_a(x_1)\bar{q}_a(x_2) + \bar{q}_a(x_1)q_a(x_2)]. \tag{5}$$

Here $q_a(x)$ are the quark or antiquark structure functions of the two colliding hadrons evaluated at momentum fractions x_1 and x_2. The sum is over quark flavors. In addition, one has the kinematic relations,

$$\begin{aligned} \tau &\equiv x_1 x_2 = M^2/s, \\ x_F &= x_1 - x_2, \end{aligned} \tag{6}$$

where M is the invariant mass of the lepton pair and s is the square of the center-of-mass energy. The cross section is proportional to α^2, indicating its electromagnetic character.

Eq. 5 shows that the antiquark distribution enters as a multiplicative term in the DY cross section rather than an additive term in the DIS cross section. Hence, the antiquark distributions can be sensitively determined in the DY experiments. The dimuon data from the FNAL E288, in which the Υ resonances were discovered [38], were analysed [39] to extract the sea quark distribution in the nucleon. By assuming a flavor-symmetric nucleon sea, namely, $\bar{u}(x) = \bar{d}(x) = \bar{s}(x) = Sea(x)$, the dimuon mass distribution obtained in 400 GeV proton-nucleus interaction was described by $xSea(x) = 0.6x^{-10}$. In a later analysis [40] containing additional data at 200 and 300 GeV, E288 collaboration found that a much better fit could be obtained with an asymmetric sea, namely,

$$\bar{u}(x) = (1-x)^{3.48}\bar{d}(x), \qquad \bar{s}(x) = (\bar{u}(x) + \bar{d}(x))/4. \tag{7}$$

The need for an asymmetric $\bar{u}$ and $\bar{d}$ was also manifested in the E288 $d\sigma/dy$ data [40] at $y = 0$, where y is the center-of-mass rapidity. For $p + A$ collision, $d\sigma/dy$ at $y = 0$ is expected to be positive due to the excess of u over d valence quarks in the proton. The E288 data showed that the slopes are indeed positive, but larger than expected from a flavor symmetric sea. A surplus of $\bar{d}$ over $\bar{u}$ in the proton sea would lead to more positive slope in agreement with the data [40].

The FNAL E439 collaboration [41] studied high mass dimuons produced in $p + W$ interaction at 400 GeV. Their spectrometer covered a considerably larger range in x_F than E288. They again found that an asymmetric sea, $\bar{u}(x) = (1-x)^{2.5}\bar{d}(x)$, can well describe their data.

With all the tantalizing evidence for an asymmetric sea from DIS and DY experiments, it is curious that all global analyses [31, 32, 33, 34, 35] of parton distributions in the 1980's still assumed a symmetric light-quark sea. This probably reflected the reluctance to adopt an unconventional description of the nucleon sea without compelling and unambiguous experimental evidences. As discussed in the next Section, such evidences became available in the 1990's.

3. RECENT EXPERIMENTAL DEVELOPMENTS

3.1 NMC Measurements of the Gottfried Integral

After the discovery of the so-called 'EMC effect' [42] which showed that the parton distribution in a nucleus is different from that in the deuteron, the EMC detector system was modified by the New Muon Collaboration (NMC) to study in detail the EMC effect. Special emphases were placed by the NMC on the capability to explore low-x region where the 'shadowing effect' [43] is important, and on accurate measurements of cross section ratios [44]. By implementing a 'small angle' trigger which extended the scattering angle coverage down to 5 mrad, the lowest value of x reached by NMC was ~ 0.001. The NMC also placed two targets in the muon beam, allowing DIS data from two different targets to be recorded simultaneously, thus greatly reducing the beam flux normalization uncertainty. To account for the different geometric acceptances for events originating from the two targets, half of the data were taken using a different target configuration where the locations of the two targets were interchanged.

The upgraded NMC detectors allowed a definitive study [45] of the shadowing effect at low x. Moreover, they enabled a much more accurate determination of the Gottfried integral. Figure 2 shows the $F_2^p - F_2^n$ reported by the NMC in 1991 [46], in which the smallest x reached (0.004) was significantly lower than in previous experiments. Taking advantage of their accurate measurements of the F_2^n/F_2^p ratios, NMC used the following expression to evaluate $F_2^p - F_2^n$, namely,

$$F_2^p - F_2^n = 2\ F_2^d\ (1 - F_2^n/F_2^p)/(1 + F_2^n/F_2^p). \tag{8}$$

The ratio $F_2^n/F_2^p \equiv 2F_2^d/F_2^p - 1$ was determined from NMC's F_2^d/F_2^p measurement, while F_2^d was taken from a fit to previous DIS experiments at SLAC [47], Fermilab [27], and CERN [48, 49]. The value of the Gottfried integral for the measured region at $Q^2 = 4$ GeV^2 is $S_G(0.004 - 0.8) = 0.227 \pm 0.007(stat) \pm 0.014(syst)$. The contribution to S_G from $x > 0.8$ was estimated to be 0.002 ± 0.001. Assuming that $F_2^p - F_2^n$ at $x < 0.004$ behaves as ax^b, NMC obtained $S_G(0 - 0.004) = 0.011 \pm 0.003$. Summing the contributions from all regions of x, NMC obtained $S_G = 0.240 \pm 0.016$, which was significantly below 1/3. This represented the best evidence thus far that the GSR was indeed violated.

In 1994, NMC reevaluated [50] the Gottfried integral using a new F_2^d parametrization from Ref. [51] and newly determined values of F_2^d/F_2^p. The new F_2^d parametrization include data from SLAC [47], BCDMS [48], as well as NMC's own measurement [51]. The new NMC results for $F_2^p - F_2^n$ are shown in Figure 2. Note that the 1994 values are slightly larger (smaller) than the 1991 values at small (large) x. The new evaluation gave $S_G(0.004 - 0.8) = 0.221 \pm 0.008(stat) \pm 0.019(syst)$, and the Gottfried integral became

$$S_G = 0.235 \pm 0.026. \tag{9}$$

This value is consistent with the earlier number. The new systematic error is larger than the old one, reducing somewhat the overall significance of the NMC measurement. Nevertheless, the violation of the GSR is established at a 4σ level.

More recently, NMC published their final analysis of F_2^d/F_2^p [52] and F_2^d [53, 54]. This analysis includes the 90 and 280 GeV data taken in 1986 and 1987, as well as the 1989 data at 120, 200 and 280 GeV. The 1989 data were not used in the earlier evaluations [46, 50] of the Gottfried integral. Based on these new data, NMS reported a Gottfried integral in the interval $0.004 < x < 0.8$ of $0.2281 \pm 0.0065(stat)$ at $Q^2 = 4$ GeV^2 [52]. This agrees within statistical errors with previous NMC results [46, 50].

3.2 E772 Drell-Yan Experiment

The main physics goal of the Fermilab experiment 772 was to examine the origin of the EMC effect. Among the many theoretical models which explain the EMC effect [55], the pion-excess model [56] predicted a large enhancement of antiquark content due to the presence of additional meson cloud in heavy nuclei. This prediction could be readily tested by measuring the nuclear dependence of proton-induced DY cross sections. Using an 800 GeV proton beam, the DY cross section ratios of a number of nuclear targets (C, Ca, Fe, W) were measured [57] relative to deuterium with high statistics over the region $0.04 < x_2 < 0.35$. While the enhancement of antiquark contents predicted by the pion-excess model was not observed, the E772 results are in good agreement with the prediction of the rescaling model [58].

Information on the $\bar{d}/\bar{u}$ asymmetry has also been extracted from the E772 data [59]. At $x_F > 0.1$, the dominant contribution to the proton-induced DY cross section comes from the annihilation of u quark in the projectile with the $\bar{u}$ quark in the target nucleus. It follows that the DY cross section ratio of a non-isoscalar target (like $^1H, Fe, W$) over an isoscalar target (like $^2H,^{12}C,^{40}Ca$) is given as

$$R_A(x_2) \equiv \sigma_A(x_2)/\sigma_{IS}(x_2) \approx 1 + [(N-Z)/A][(1-\bar{u}(x_2)/\bar{d}(x_2))/(1+\bar{u}(x_2)/\bar{d}(x_2))], \quad (10)$$

where x_2 is the Bjorken-x of the target partons, IS stands for isoscalar, and N, Z and A refer to the non-isoscalar target. The $(N-Z)/A$ factor in Eq. 10 shows that the largest sensitivity to the $\bar{d}/\bar{u}$ could be obtained with a measurement of $\sigma(p+p)/\sigma(p+d)$. Nevertheless, for W target $(N-Z)/A = 0.183$ and the E772 σ_W/σ_{IS} data could still be used to study the $\bar{d}, \bar{u}$ asymmetry.

Figure 3 shows the E772 DY cross section ratios from the neutron-rich W target over the isoscalar targets, ^2H and ^{12}C. Corrections have been applied to the two data points at $x_2 < 0.1$ to account for the nuclear shadowing effects in C and W [59]. The E772 data provided some useful constraints on the $\bar{d}/\bar{u}$ asymmetry. In particular, some early parametrizations [60, 61] of large $\bar{d}/\bar{u}$ asymmetry were ruled out. Despite the relatively large error bars, Figure 3 shows $R > 1.0$ at $x_2 > 0.15$, suggesting that $\bar{d} > \bar{u}$ in this region.

E772 collaboration also presented the DY differential cross sections for $p+d$ at $\langle M_{\mu\mu}\rangle =$ 8.15 GeV. As shown in Figure 4, the DY cross sections near $x_F = 0$ are sensitive to $\bar{d}/\bar{u}$ and the data disfavor a large $\bar{d}/\bar{u}$ asymmetry. Figure 4 also shows that a recent parton distribution function, MRST [62], which has modest $\bar{d}/\bar{u}$ asymmetry, is capable of describing the $p+d$ differential cross sections well (see Section 3.6).

While the E772 data provide some useful constraints on the values of $\bar{d}/\bar{u}$, it is clear that a measurement of $\sigma_{DY}(p+d)/\sigma_{DY}(p+p)$ is highly desirable. The $(N-Z)/A$ factor is now equal to -1, indicating a large improvement in the sensitivity to $\bar{d}/\bar{u}$. Moreover, the uncertainty arising from nuclear effects would be much reduced. It has been pointed out [63] that $\bar{d}/\bar{u}$ asymmetry in the nucleon could be significantly modified in heavy nuclei through recombination of partons from different nucleons. Clearly, an ideal approach is to first determine $\bar{d}/\bar{u}$ in the nucleon before extracting the $\bar{d}/\bar{u}$ information in heavy nuclei.

3.3 NA51 Drell-Yan Experiment

Following the suggestion of Ellis and Stirling [60], the NA51 collaboration at CERN carried out the first dedicated dimuon production experiment to study the flavor structure of the nucleon sea [64]. Using a 450 GeV/c proton beam, roughly 2800 and 3000 dimuon events with $M_{\mu\mu} > 4.3$ GeV have been recorded, respectively, for $p+p$ and $p+d$ interaction. The spectrometer setting covers the kinematic region near $y = 0$. At $y = 0$, the asymmetry parameter, A_{DY}, is given as

$$A_{DY} \equiv \frac{\sigma^{pp} - \sigma^{pn}}{\sigma^{pp} + \sigma^{pn}} \approx \frac{(4\lambda_V - 1)(\lambda_s - 1) + (\lambda_V - 1)(\lambda_s - 1)}{(4\lambda_V + 1)(\lambda_s + 1) + (\lambda_V + 1)(\lambda_s + 1)}, \tag{11}$$

where $\lambda_V = u_V/d_V$ and $\lambda_s = \bar{u}/\bar{d}$. In deriving Eq. 11, the negligible sea-sea annihilation was ignored and the validity of charge symmetry was assumed. At $x = 0.18$, $\lambda_V \approx 2$ and according to Eq. 11 $A_{DY} = 0.09$ for a symmetric sea, $\lambda_s = 1$. For an asymmetric $\bar{d} > \bar{u}$ sea, A_{DY} would be less than 0.09.

From the DY cross section ratio, σ^{pp}/σ^{pd}, NA51 obtained $A_{DY} = -0.09 \pm 0.02(stat) \pm 0.025(syst)$. This then led to a determination of $\bar{u}/\bar{d} = 0.51 \pm 0.04(stat) \pm (syst)$ at $x = 0.18$ and $\langle M_{\mu\mu} \rangle = 5.22$ GeV. This important result established the asymmetry of the quark sea at a single value of x. What remained to be done was to map out the x-dependence of this asymmetry. This was subsequently carried out by the Fermilab E866 collaboration, as described in the next Section.

3.4 E866 Drell-Yan Experiment

At Fermilab, a DY experiment (E866) aimed at a higher statistical accuracy and a much wider kinematic coverage than the NA51 experiment was recently completed [65]. This experiment measured the DY muon pairs from 800 GeV proton interacting with liquid deuterium and hydrogen targets. A proton beam with up to 2×10^{12} protons per 20 s spill bombarded one of three identical 50.8 cm long cylindrical target flasks containing either liquid hydrogen, liquid deuterium or vacuum. The targets alternated every few beam spills in order to minimize time-dependent systematic effects. The dimuons accepted by a 3-dipole magnet spectrometer were detected by four tracking stations. An integrated flux of 1.3×10^{17} protons was delivered for this measurement.

Over 330,000 DY events were recorded in E866, using three different spectrometer settings which covered the regions of low, intermediate and high mass muon pairs. The data presented here are from the high mass setting, with over 140,000 DY events. Analysis of the full data sets has been completed and the results [66] are in good qualitative agreement with the high-mass data. The DY cross section ratio per nucleon for $p + d$ to that for $p + p$ is shown in Figure 5 as a function of x_2. The acceptance of the spectrometer was largest for $x_F = x_1 - x_2 > 0$. In this kinematic regime the DY cross section is dominated by the annihilation of a beam quark with a target antiquark. To a very good approximation the DY cross section ratio at positive x_F is given as

$$\sigma_{DY}(p+d)/2\sigma_{DY}(p+p) \simeq (1 + \bar{d}(x_2)/\bar{u}(x_2))/2. \tag{12}$$

In the case that $\bar{d} = \bar{u}$, the ratio is 1. Figure 5 shows that the DY cross section per nucleon for $p + d$ clearly exceeds $p + p$, and it indicates an excess of $\bar{d}$ with respect to $\bar{u}$ over an appreciable range in x_2.

Figure 5 also compares the data with next-to-leading order (NLO) calculations of the cross section ratio using the CTEQ4M [67], MRS(R2) [68], and a modified CTEQ4M parton distributions. The modified CTEQ4M parton distributions, in which the $\bar{d}+\bar{u}$ parametrization was maintained but $\bar{d}$ was set identical to $\bar{u}$, were used to illustrate the cross section ratio expected for a symmetric $\bar{d}/\bar{u}$ sea. The E866 data clearly show that $\bar{d} \neq \bar{u}$. The data are in reasonable agreement with the unmodified CTEQ4M and the MRS(R2) predictions for $x_2 < 0.15$. Above $x_2 = 0.15$ the data lie well below the CTEQ4M and the MRS(R2) values.

Using an iterative procedure described in [65, 69], values for $\bar{d}/\bar{u}$ were extracted by the E866 collaboration at $Q^2 = 54$ GeV^2 and shown in Figure 6. At $x < 0.15$, $\bar{d}/\bar{u}$ increases linearly with x and is in good agreement with the CTEQ4M and MRS(R2) parametrization. However, a distinct feature of the data, not seen in either parametrization of the parton distributions, is the rapid decrease towards unity of the $\bar{d}/\bar{u}$ ratio beyond $x_2 = 0.2$. The result from NA51 is also shown in Figure 6 for comparison.

The $\bar{d}/\bar{u}$ ratios measured in E866, together with the CTEQ4M values for $\bar{d} + \bar{u}$, were used to obtain $\bar{d} - \bar{u}$ over the region $0.02 < x < 0.345$ (Figure 7). As a flavor non-singlet quantity, $\bar{d}(x) - \bar{u}(x)$ is decoupled from the effects of the gluons and is a direct measure of the contribution from non-perturbative processes, since perturbative processes cannot cause a significant $\bar{d}$, $\bar{u}$ difference. From the results shown in Figure 7, one can obtain an independent determination [69] of the integral of $\bar{d}(x) - \bar{u}(x)$ and compare it with the NMC result (Eq. 9). E866 obtains a value $\int_0^1 \left[\bar{d}(x) - \bar{u}(x)\right] dx = 0.100 \pm 0.007 \pm 0.017$, which is 2/3 the value deduced by NMC [50].

The E866 data also allow the first determination of the momentum fraction carried by the difference of $\bar{d}$ and $\bar{u}$. One obtains $\int_{0.02}^{0.345} x \left[\bar{d}(x) - \bar{u}(x)\right] dx = 0.0065 \pm 0.0010$ at $Q^2 = 54$ GeV^2. If CTEQ4M is used to estimate the contributions from the unmeasured x regions, one finds that $\int_0^1 x \left[\bar{d}(x) - \bar{u}(x)\right] dx = 0.0075 \pm 0.0011$. Unlike the integral of $\bar{d}(x) - \bar{u}(x)$, the momentum integral is Q^2-dependent and decreases as Q^2 increases. The Q^2-dependence of the momentum fraction carried by various partons are shown in Figure 8. The calculation uses both the MRS(R2) and the new MRST [62] parton distributions for comparison.

3.5 HERMES Semi-Inclusive Experiment

It has been recognized for some time that semi-inclusive DIS could be used to extract the flavor dependence of the valence quark distributions [70]. From quark-parton model, the semi-inclusive cross section, σ_N^h, for producing a hadron on a nucleon is given by

$$\frac{1}{\sigma_N(x)} \frac{d\sigma_N^h(x,z)}{dz} = \frac{\sum_i e_i^2 f_i(x) D_i^h(z)}{\sum_i e_i^2 f_i(x)}, \tag{13}$$

where $D_i^h(z)$ is the fragmentation function signifying the probability for a quark of flavor i fragmenting into a hadron h carrying a fraction z of the initial quark energy. e_i and f_i are the charge and the distribution function of quark i, and $\sigma_N(x)$ is the inclusive DIS cross section. Assuming charge symmetry for the fragmentation functions and parton distribution functions, one can derive the relationship

$$\frac{d_v(x)}{u_v(x)} = \frac{4R^\pi(x)+1}{4+R^\pi(x)}, \tag{14}$$

where

$$R^\pi(x) = (d\sigma_n^{\pi^+}(x,z)/dz - d\sigma_n^{\pi^-}(x,z)/dz)/(d\sigma_p^{\pi^+}(x,z)/dz - d\sigma_p^{\pi^-}(x,z)/dz). \tag{15}$$

Based on a large number of semi-inclusive charged-hadron events in muon DIS from hydrogen and deuterium targets, EMC extracted [71] the values of $d_v(x)/u_v(x)$ over the range $0.028 < x < 0.66$. The EMC result agrees with neutrino measurements [72, 73] using a different method, and it demonstrates the usefulness of such semi-inclusive measurements for extracting information on valence quark distributions.

Soon after the report of GSR violation by the NMC, Levelt, Mulders and Schreiber [74] pointed out that semi-inclusive DIS could also be used to study the flavor dependence of sea quarks. In particular,

$$\frac{\bar{d}(x)-\bar{u}(x)}{u(x)-d(x)} = \frac{J(z)[1-r(x,z)]-[1+r(x,z)]}{J(z)[1-r(x,z)]+[1+r(x,z)]}, \tag{16}$$

where

$$r(x,z) = \frac{d\sigma_p^{\pi^-}(x,z)/dz - d\sigma_n^{\pi^-}(x,z)/dz}{d\sigma_p^{\pi^+}(x,z)/dz - d\sigma_n^{\pi^+}(x,z)/dz}, \quad J(z) = \frac{3}{5}\,\frac{1+D_u^{\pi^-}(z)/D_u^{\pi^+}(z)}{1-D_u^{\pi^-}(z)/D_u^{\pi^+}(z)}. \tag{17}$$

Unlike the situation for $d_v(x)/u_v(x)$ which is completely independent of the fragmentation functions D_i^h, Eq. 16 shows that fragmentation functions are needed to extract the values of $\bar{d}(x)-\bar{u}(x)$.

Very recently, the HERMES collaboration [75] at DESY reported their measurements of charged hadrons produced in the scattering of a 27.5 GeV positron beam on internal hydrogen, deuterium, and ^{3}He target. The fragmentation functions $D_i^{\pi^\pm}(z)$ were extracted from the ^{3}He data, while the hydrogen and deuterium data allowed a determination of $r(x,z)$. The values of $(\bar{d}-\bar{u})/(u-d)$ show no z dependence and are positive over the region $0.02 < x < 0.3$, showing clearly an excess of $\bar{d}$ over $\bar{u}$. Using the GRV94 LO [76] parametrization of $u(x)-d(x)$, the HERMES collaboration obtained $\bar{d}(x)-\bar{u}(x)$ as shown in Figure 7. The integral of $\bar{d}-\bar{u}$ over the measured x region gives $\int_{0.02}^{0.3}\left[\bar{d}(x)-\bar{u}(x)\right]dx = 0.107 \pm 0.021(stat) \pm 0.017(syst)$. The total integral over all x is extrapolated to be 0.16 ± 0.03, consistent with the result from NMC. It is gratifying that the results from E866 and HERMES are in rather good agreement, even though these two experiments use very different methods and cover very different Q^2 values ($Q^2 = 54$ GeV^2 in E866 and $Q^2 = 2.3$ GeV^2 in HERMES).

It should be mentioned that semi-inclusive DIS could be extended [77, 78] to situations involving polarized lepton beam and polarized targets in order to study the flavor dependence of the spin-dependent structure functions. Both the Spin Muon Collaboration (SMC) [79] and the HERMES Collaboration [80] have reported the polarized valence quark distributions, $\Delta u_v(x)$ and $\Delta d_v(x)$, and the non-strange sea-quark polarization, $\Delta\bar{q}(x)$.

3.6 Impact on the Parton Distribution Functions

Since evidences for a flavor asymmetric sea were reported by the NMC and NA51, several groups [67, 68, 76] performing global analysis of parton distribution function (PDF) have all required $\bar{d}$ to be different from $\bar{u}$. The NMC result constrained the integral of the $\bar{d}-\bar{u}$ to be 0.149 ± 0.039, while the NA51 result requires $\bar{d}/\bar{u}$ to be 1.96 ± 0.13 at $x = 0.18$. Clearly, the x dependences of $\bar{d}-\bar{u}$ and $\bar{d}/\bar{u}$ were undetermined. Figures 9 and 10 compare the E866 measurements of $x(\bar{d}-\bar{u})$ and $\bar{d}/\bar{u}$ with the parametrizations of the MRS(R2) [68], CTEQ4M [67], and GRV94 [76], three of the most frequently used PDF's prior to E866's measurement.

Recently, several PDF groups published new parametrizations taking into account of new experimental information including the E866 data. The parametrization of the x dependence of $\bar{d}-\bar{u}$ is now strongly constrained by the E866 and HERMES data. In particular, $\bar{d}(x)-\bar{u}(x)$ or $\bar{d}(x)/\bar{u}(x)$ are parametrized as follows;

MRST [62]:

$$\bar{d}(x) - \bar{u}(x) = 1.29x^{0.183}(1-x)^{9.808}(1 + 9.987x - 33.34x^2),\ Q_0^2 = 1\ GeV^2,$$

GRV98 [81]:

$$\bar{d}(x) - \bar{u}(x) = 0.20x^{-0.57}(1-x)^{12.4}(1 - 13.3x^{0.5} + 60.0x),\ Q_0^2 = 0.4\ GeV^2,$$

CTEQ5M [82, 83]:

$$\bar{d}(x)/\bar{u}(x) = 1 - 1.095x + 3.159x^{0.5}/[1 + ((x - 0.188)/0.116)^2],\ Q_0^2 = 1\ GeV^2. \tag{18}$$

As shown in Figure 10, these new parametrizations give significantly different shape for $\bar{d}/\bar{u}$ at $x > 0.15$ compared to previous parametrizations. Table 1 also lists the values of $\bar{d}-\bar{u}$ integral from various recent PDF's.

It is interesting to note that the E866 data also affect the parametrization of the valence-quark distributions. Figure 11 shows the NMC data for $F_2^p - F_2^n$ at $Q^2 = 4$ GeV^2, together with the fits of MRS(R2) and MRST. It is instructive to decompose $F_2^p(x) - F_2^n(x)$ into contributions from valence and sea quarks:

$$F_2^p(x) - F_2^n(x) = \frac{1}{3}x\left[u_v(x) - d_v(x)\right] + \frac{2}{3}x\left[\bar{u}(x) - \bar{d}(x)\right]. \tag{19}$$

As shown in Figure 11, the E866 data provide a direct determination of the sea-quark contribution to $F_2^p - F_2^n$. In order to preserve the fit to $F_2^p - F_2^n$, the MRST's parametrization for the valence-quark distributions, $u_v - d_v$, is significantly lowered in the region $x > 0.01$. Indeed, one of the major new features of MRST is that d_v is now significantly higher than before at $x > 0.01$. Although the authors of MRST attribute this to the new W-asymmetry data from CDF [84] and the new NMC results on F_2^d/F_2^p [52], it appears that the new information on $\bar{d}(x) - \bar{u}(x)$ has a direct impact on the valence-quark distributions too.

Another implication of the E866 data is on the behavior of $F_2^p - F_2^n$ at small x. In order to satisfy the constraint $\int_0^1 [u_v(x) - d_v(x)]dx = 1$, the MRST values of $u_v(x) - d_v(x)$ at $x < 0.01$ are now much larger than in MRS(R2), since $u_v(x) - d_v(x)$ at $x > 0.01$ are smaller than before. As a consequence, $F_2^p - F_2^n$ is increased at small x and MRST predicts a large contribution to the Gottfried integral from the small-x ($x < 0.004$) region, as shown in Figure 12. If the MRST parametrization for $F_2^p - F_2^n$ at $x < 0.004$ were used, NMC would have deduced a value of 0.252 for the Gottfried integral, which would imply a value of 0.122 for the $\bar{d} - \bar{u}$ integral. This would bring better agreement between the E866 and the NMC results on the $\bar{d} - \bar{u}$ integral.

3.7 Comparison Between Various Measurements

Are the various measurements of sea quark flavor asymmetry consistent among them? In particular, is the E866 result consistent with the earlier E772 and the NA51 DY experiments, and with the HERMES and NMC DIS measurements? To address this question, we first compare E866 with E772, both of which are DY experiments using 800 GeV proton beam with essentially the same spectrometer. Figures 3 and 4 show that the MRST parton distributions, which determined $\bar{d} - \bar{u}$ based on the E866 data, can also describe the E772 data very well, and we conclude that the E866 and E772 results are consistent.

Although both NA51 and E866 measured $\sigma(p+d)/2\sigma(p+p)$ to extract the values of $\bar{d}/\bar{u}$, some notable differences exist. As mentioned earlier, NA51 measured the ratio at a single value of x_2 ($x_2 = 0.18$) near $x_F \approx 0$ using 450 GeV proton beam, while E866 used 800 GeV proton beam to cover a broader range of x_2 at $x_F > 0$. It is instructive to compare the NA51 result at $x_2 = 0.18$ with the E866 data at $x_2 = 0.182$. Table 2 lists the kinematic variables and physics quantities derived from these two data points. It is interesting to note that the values of $\sigma(p+d)/2\sigma(p+p)$ at $x_2 = 0.18$ are actually very similar for NA51 and E866, even though the derived values for $\bar{d}/\bar{u}$ differ significantly. This reflects the difference in x_F for both experiments, making the values of $\bar{d}/\bar{u}$ extracted from $\sigma(p+d)/2\sigma(p+p)$ different. The other difference is Q^2, being a factor of 3.6 higher for E866. Using MRST and CTEQ5M to estimate the Q^2 dependence of $\bar{d}/\bar{u}$, we find that the NA51 value of $\bar{d}/\bar{u}$ is reduced by ≈ 3 % going from $Q^2 = 27.2$ GeV^2 to $Q^2 = 98.0$ GeV^2. This brings slightly better agreement bewteen NA51 and E866.

The methods used by HERMES and E866 to determine $\bar{d} - \bar{u}$ are totally different, and it is reassuring that the results came out alike, as shown in Figure 7. The $\bar{d} - \bar{u}$ values from HERMES are in general somewhat larger than those of E866. At a relatively low mean Q^2 of 2.3 GeV^2, the HERMES experiment could be subject to high-twist effect [85]. Additional data from HERMES are expected to improve the statistical accuracy.

The comparison between E866 and NMC in terms of the integral of $\bar{d} - \bar{u}$ has been discussed earlier. A possible origin for the apparent differences of the integral was also discussed in Section 3.6.

4. ORIGINS OF THE $\bar{d}/\bar{u}$ ASYMMETRY

4.1 Pauli Blocking

The earliest experiments indicated that the value of the Gottfried integral might be less than 1/3, leading to speculation regarding the origin of this reduction. Field and Feynman suggested [24] that it could be due to Pauli blocking in so far as $u\bar{u}$ pairs would be suppressed relative to $d\bar{d}$ pairs because of the presence of two u-quarks in proton as compared to a single d-quark. Ross and Sachrajda [86] questioned that this effect would be appreciable because of the large phase-space available to the created $q\bar{q}$ pairs. They also showed that perturbative QCD would not produce a $\bar{d}$, $\bar{u}$ asymmetry. Steffens and Thomas [87] recently looked into this issue, explicitly examining the consequences of Pauli blocking. They similarly concluded that the blocking effects were small, particularly when the antiquark is in a virtual meson.

The small d, u mass difference (actually, $m_d > m_u$) of 2 to 4 MeV compared to the nucleon confinement scale of 200 MeV/c does not permit any appreciable difference in their relative production by gluons. At any rate, one observes a surplus of $\bar{d}$ which is the heavier of the two species. As pointed out above, blocking effects arising from the Pauli exclusion principle should also have little effect. Thus another, presumably non-perturbative, mechanism must be found to account for the large measured $\bar{d}, \bar{u}$ asymmetry.

4.2 Meson-Cloud Models

A natural origin for this flavor asymmetry is the virtual states of the proton containing isovector mesons. This point appears to have first been made by Thomas in a publication [88] treating SU(3) symmetry breaking in the nucleon sea. Sullivan [89] had earlier shown that virtual meson-baryon states directly contribute to the nucleon's structure function. A large number of authors have contributed to calculating the asymmetry from this perspective, so recent reviews [90, 91] should be consulted for a complete list of contributions.

Conservation of electric charge and isospin naturally creates a flavor asymmetry when isovector mesons are involved. For example the Fock decomposition of the proton into its πN components yields

$$|p\rangle \rightarrow \sqrt{\frac{1}{3}}\ |p_0\pi^0\rangle + \sqrt{\frac{2}{3}}\ |n_0\pi^+\rangle, \tag{20}$$

where p_0 and n_0 are regarded as proton and neutron states with symmetric seas. The $\bar{d}/\bar{u}$ ratio for the configurations shown in Eq. 20 is 5! Thus the presence of such virtual states can readily generate a large flavor asymmetry. If allowing for the possibility of $\pi\Delta$ configurations it is easy to show that the integrated $\bar{d}, \bar{u}$ difference in the proton is given by

$$\int_0^1 [\bar{d}(x) - \bar{u}(x)]dx = \frac{1}{3}(2a - b), \tag{21}$$

where $a(b)$ is the probability of $\pi N(\pi\Delta)$ component in the proton. The value extracted from

E866 for the above integral is 0.100 ± 0.018, leading to $a = 0.2 \pm 0.036$ if one accepts $b \approx a/2$ as found in many calculations.

Many attempts [92, 93, 94, 95, 96, 97, 98] have been made to calculate the flavor asymmetry due to isovector mesons. Most start with the following convolution expressions:

$$|p\rangle = a_0|p_0\rangle + \sum_{MB} a^p_{MB}|M\rangle|B\rangle, \tag{22}$$

$$x\bar{q}_p(x, Q^2) = \sum_{MB} a^p_{MB} \int_x^1 dy\ f_{MB}(y)\ \frac{x}{y}\ \bar{q}_M(\frac{x}{y}, Q^2), \tag{23}$$

where

$$f_{MB}(y) = \frac{g^2_{MpB}}{16\pi^2} y \int_{-\infty}^{t_{min}} dt \frac{F(t, m_p, m_B)}{(t - m^2_M)^2} F^2_{MpB}(t, \Lambda), \quad t_{min} = m^2_p y - m^2_B \frac{y}{1-y}. \tag{24}$$

In the above expressions x is the fraction of proton's momentum carried by the antiquark, and y is fraction carried by the meson (M). The meson-proton-baryon couplings are characterized by coupling constants g_{MpB}, and form factors $F_{MpB}(t, \Lambda)$ where Λ is a cutoff parameter. $F(t, m_p, m_B)$ is a kinematic factor depending on whether B is in the baryon octet or decuplet. As pions are the only mesons usually considered and the baryons are usually restricted to nucleons and deltas, the coupling constants are well known and the partonic structure of the pion, $\bar{q}_\pi(x, Q^2)$, is fixed by measurement of the DY process using high energy pion beams. The only uncertainties are the form factors $F_{\pi pN}(t)$ and $F_{\pi p\Delta}(t)$. One attempts to determine these form factors by using [99, 100] the measured yields from a variety of high energy hadronic reactions at small p_T such as $p + p \to n + X$ and $p + p \to \Delta^{++} + X$. Even though there is a sizable amount of available data, employing such a procedure does not produce a precise result. The cutoff parameters used in the extracted form factors are of the order of 1 GeV but the uncertainties in their values produce factors of two in predicted antiquark contents in the nucleons.

Even though calculated value of the integral of $\bar{d}(x) - \bar{u}(x)$ is often in agreement with experiment, it is not possible to achieve a quantitative fit to the measured x dependence of the difference [69]. Figure 7 compares $\bar{d}(x) - \bar{u}(x)$ from E866 with a pion-cloud model calculation, following the procedure detailed by Kumano [93]. A dipole form, with $\Lambda = 1.0$ GeV for the πNN form factor and $\Lambda = 0.8$ GeV for the $\pi N\Delta$ form factor, was used. Calculations of $\bar{d}(x)/\bar{u}(x)$ are even more unsuccessful, as knowledge of the x dependence of the symmetric sea is required in this instance [69].

It is instructive to compare the pion-model prediction with the current PDF parametrization of $x(\bar{d} + \bar{u})$. Figure 13 shows that at small x $(x < 0.1)$ the valence quarks in the pion cloud account for less than 1/3 of the $\bar{d} + \bar{u}$ contents in the proton. In contrast, at large x $(x > 0.5)$ $\bar{d} + \bar{u}$ can be entirely attributed to the pion cloud.

More recent attempts [99, 100] to calculate the asymmetry due to isovector mesons find a smaller $\pi\Delta$ component in the nucleon than is presented following Eq. 21. The πN component is still about 20% while the $\pi\Delta$ piece is down around 6%. As a result the integrated asymmetry is too large, typically 0.16. However considerable progress has been made by Reggeizing the virtual mesons [100]. This procedure has two interesting consequences, first it shows that the principal contributions to the asymmetry come from virtual pions and secondly it reduces the contributions from these pions at large x, allowing the ratio $\bar{d}(x)/\bar{u}(x)$ to approach 1 for $x > 0.3$.

4.3 Chiral Models

An alternative approach [61, 101, 102, 103] also employing virtual pions to produce the $\bar{d}, \bar{u}$ asymmetry uses constituent quarks and pions as the relevant degrees of freedom. Such models are usually referred to as chiral models [104]. In this model, a portion of the sea comes from the couplings of Goldstone bosons to the constituent quarks, such as $u \to d\pi^+$ and $d \to u\pi^-$. The excess of $\bar{d}$ over $\bar{u}$ is then simply due to the additional up valence quark in the proton.

The chiral models have less dynamical freedom, and the meson-baryon expansion can be shown to predict $\bar{d}(x)/\bar{u}(x) < 11/7$ independent of x or Q^2. This limit is exceeded for $0.12 < x < 0.2$ as shown in Figure 6. The limit on the maximum value of the ratio can be traced to the fact that there is no mechanism to suppress virtual $\pi\Delta$-like configurations which are seen in Eq. 21 to reduce the asymmetry. Some extensions of the simple chiral quark model can obtain agreement with certain features of the observed asymmetry but only with the introduction of additional parameters. A calculation [69, 105] of $\bar{d}(x) - \bar{u}(x)$ (Figure 7) yielded too soft a distribution relative to experiment, indicating [69] that more dynamics must be included in the chiral quark model if it is to produce more than rough qualitative agreement with the observed asymmetry in the up, down sea of the nucleon.

4.4 Instanton Models

Instantons have been known as theoretical constructs since the seventies [106, 107, 108]. They represent non-perturbative fluctuations of the gauge fields that induce transitions between degenerate ground states of different topology. In the case of QCD, the collision between a quark and an instanton flips the helicity of the quark while creating a $q\bar{q}$ pair of different flavor. Thus, interaction between a u quark and an instanton results in a u quark of opposite helicity and either a $d\bar{d}$ or $s\bar{s}$ pair. Such a model has the possibility of accounting for both the flavor asymmetry and the "spin crisis". However, the model has been little used for this purpose. There is only one case [109] of its being employed to explain these anomalous effects. In the case of the $\bar{d}, \bar{u}$ flavor asymmetry the authors of ref. [109] fit the instanton parameters to reproduce the violation of the GSR observed by NMC. The prediction [109] at large x, $\bar{d}(x)/\bar{u}(x) \to 4$, is grossly violated by experiment (see Figure 6). Thus, it appears that while instantons have the possibility for accounting for flavor and spin anomalies, the approach is not yet sufficiently developed for a direct comparison. The final state created via an instanton collision is quite similar to that created via the emission of meson in the chiral model.

4.5 Charge Symmetry Violation

Charge symmetry is believed to be well respected in strong interaction. Extensive experimental searches for charge symmetry violation (CSV) effects in various nuclear processes reveal an amount on the order of 0.3% [110]. This is consistent with the expectation that CSV effects are caused by electromagnetic interaction and by the small mass difference between the u and d quarks [111].

It has been generally assumed that the parton distributions in hadrons obey charge symmetry. This assumption enables one to relate the parton distributions in the proton and neutron in a simple fashion, $u_p(x) = d_n(x), d_p(x) = u_n(x)$, etc. Indeed, charge symmetry is usually assumed in the analysis of DIS and DY experiments, which often use nuclear targets containing both protons and neutrons. Charge symmetry is also implicit in the derivation of many QCD sum rules, including the Gottfried sum rule, the Adler sum rule, and the Bjorken sum rule.

The possibility that charge symmetry could be significantly violated at the parton level has been discussed recently by several authors [112, 113, 114, 115, 116, 117, 118]. Ma and collaborators [112, 113] pointed out that the violation of the GSR can be caused by CSV as well as by flavor asymmetry of the nucleon sea. They also showed that DY experiments, such as NA51 and E866, are subject to both flavor asymmetry and CSV effects. Using the bag model, Rodionov et al [116] showed that a significant CSV effect of $\sim 5\%$ could exist for the "minority valence quarks" [i.e. $d_p(x)$ and $u_n(x)$] at large x ($x > 0.4$). A model study [118] of CSV for sea quarks shows that the effect is very small, roughly a factor of 10 less than for valence quarks. Londergan & Thomas have reviewed the role of CSV for parton distributions [119].

Recently Boros, Londergan and Thomas (BLT) [120] compared the parton distributions, $F_2^{\nu N}(x, Q^2)$ and $F_2^{\mu N}(x, Q^2)$. The $F_2^{\mu N}(x, Q^2)$ structure function extracted from DIS muon scattering is defined as

$$F_2^{\mu N}(x, Q^2) \equiv \frac{F_2^{\mu p}(x, Q^2) + F_2^{\mu n}(x, Q^2)}{2} \tag{25}$$

$$= \frac{5}{18} x[u + \bar{u} + d + \bar{d} + \frac{2}{5}(s + \bar{s}) + \frac{8}{5}(c + \bar{c})]. \tag{26}$$

In going from Eq. 25 to 26, the (x, Q^2) dependence has been suppressed and charge symmetry ($u_p = d_n = u$, etc.) has been employed. For neutrino DIS one has

$$F_2^{\nu N}(x, Q^2) = x[u + \bar{u} + d + \bar{d} + 2s + 2\bar{c}], \tag{27}$$

again using charge symmetry and suppressing the (x, Q^2) dependence in the parton distributions. Neglecting the contribution of charmed quarks in the nucleon and correcting for the small difference due to strange quark contributions one expects

$$\frac{\frac{18}{5} F_2^{\mu N}(x, Q^2)}{F_2^{\nu N}(x, Q^2)} \approx 1. \tag{28}$$

After making the necessary small corrections, BLT found that the ratio in Eq. 28 at common values of (x, Q^2) is 1 for $x > 0.1$ but for $x < 0.1$ the ratio progressively decreases below 1 as x decreases. They suggested that this effect might be due to a violation of charge symmetry in the sea of the nucleon. To achieve agreement with experiment, BLT found it necessary to set $\bar{d}_n(x) \approx 1.25\bar{u}_p(x)$ and $\bar{u}_n(x) \approx 0.75\bar{d}_p(x)$ at small x. As the total number of sea quarks is kept equal in the neutron and proton $(\bar{u}_p(x) + \bar{d}_p(x) \approx u_n(x) + \bar{d}_n(x))$, one deduces $\bar{d}_p(x) \approx \bar{u}_p(x)$ and $\bar{d}_n(x) \approx (5/3)\bar{u}_n(x)$, a most striking asymmetry between the proton and the neutron sea.

How would this claim of large CSV affect the E866 analysis of the flavor asymmetry? First, CSV alone could not account for the E866 data. In fact, an even larger amount of flavor asymmetry is required to compensate for the possible CSV effect [120]. Second, there has been no indication of CSV for $x > 0.1$. Thus, the large $\bar{d}/\bar{u}$ asymmetry from E866 for $x > 0.1$ is not affected. Fortunately, this radical alteration of the conventional view does not appear to be the case, as shown recently by Bodek et al. [121], who showed that the measured asymmetry of $W^+(W^-)$ production at CDF is consistent with charge symmetry and in strong disagreement with the suggestion of BLT. The reasons for the discrepancy of the DIS data with Eq. 28 must be found elsewhere.

5. FURTHER IMPLICATIONS OF THE MESON-CLOUD MODELS

5.1 Strange Sea of the Nucleon

Models in which virtual mesons are admitted as degrees of freedom have implications that extend beyond the $\bar{d}, \bar{u}$ flavor asymmetry addressed above. They create hidden strangeness in the nucleon via such virtual processes as $p \to \Lambda + K^+, \Sigma + K$, etc. Such processes are of considerable interest as they imply different s and $\bar{s}$ parton distributions in the nucleon, a feature not found in gluonic production of $s\bar{s}$ pairs. This subject has received a fair amount of attention in the literature [99, 122, 123, 124, 125] but experiments have yet to clearly identify such a difference. Thus in contrast to the $\bar{d}, \bar{u}$ flavor asymmetry, to date there is no positive experimental evidence for $s\bar{s}$ contributions to the nucleon from virtual meson-baryon states [19, 126].

A difference between the s and $\bar{s}$ distribution can be made manifest by direct measurement of the s and $\bar{s}$ parton distribution functions in DIS neutrino scattering, or in the measurement of the q^2 dependence of the strange quark contribution $(F^p_{1s}(q^2))$ to the proton charge form factor. This latter case is not well known and follows from a suggestion of Kaplan and Manohar [127] regarding the new information contained in the weak neutral current form factors of the nucleon. Measurement of these form factors allows extraction of the strangeness contribution to the nucleon's charge and magnetic moment and axial form factors. The portion of the charge form factor $F^p_{1s}(q^2)$ due to strangeness clearly is zero at $q^2 = 0$, but if the s and $\bar{s}$ distributions are different the form factor becomes non-zero at finite q^2. These "strange" form factors can be measured in neutrino elastic scattering [128] from the nucleon, or by selecting the parity-violating component of electron-nucleon elastic scattering, as is now being done at the Bates [129] and Jefferson Laboratories [130].

It is worth pointing out that there is a relationship between the parton distributions and the form factors of a hadron. If the neutron's charge form factor is explained in terms of a particular meson-baryon expansion, then one should expect that the expansion is consistant with the neutron's partonic structure. Little work appears to have been done bringing these descriptions together. Below is an example showing the impact of the nucleons pionic content, inferred from the flavor asymmetry, on the spin distribution in the nucleon.

5.2 Spin Dependent Structure Functions

As the pion is a $J^\pi = 0^-$ hadron it must be emitted as a p-wave requiring that the nucleon flip its spin 1/3 of the time upon emitting a pion. Thus, it appears that such a process might readily account for the reduction of g_A from 1.667 and the overall reduction in the quark contribution to nucleon spin as observed in DIS. The contribution to g_A from virtual pions is

$$g_A = \Delta u - \Delta d = \frac{5}{3} - \frac{20}{27}(2a+b) + \frac{32}{27}\sqrt{2ab} \tag{29}$$

$$= 1.53 \quad \text{for} \quad a = 0.2, b = 0.1, \tag{30}$$

and to the total nucleon spin due to up and down quarks

$$\Delta q = \Delta u + \Delta d = 1 - \frac{2}{3}(2a - b) \tag{31}$$

$$= 0.80 \quad \text{for} \quad a = 0.2, b = 0.1. \tag{32}$$

Thus, virtual pions do reduce the fraction of nucleon spin carried by up and down quarks but the effect is not sufficient to reduce g_A from its SU(6) value of 5/3 to the experimental value of 1.256. Eqs. 21 and 30, together with the values of $\bar{d} - \bar{u}$ integral determined from experiments, allow us to calculate g_A as a function of a. The different values of the $\bar{d} - \bar{u}$ integral from the NMC and E866 correspond to two different curves shown in Figure 14. Figure 14 illustrates the possible range of g_A achievable from virtual pions alone. Presumably relativistic effects are responsible for the bulk of that reduction [131]. Similarly, virtual pions reduce the total spin carried by u and d quarks but not enough to be a dominant effect as $\Delta u + \Delta d \approx 0.25$.

There is an aspect of spin distributions predicted by virtual pion emission that is present in the data. The spin carried by antiquarks in the virtual pion model must be zero. Indeed the measured value [79], $\Delta \bar{q} = 0.01 \pm 0.04 \pm 0.03$ is consistent with that picture. It is very likely that meson will prove to play an important part in understanding the nucleon's spin structure but that role is not clear at present.

5.3 Sea Quark Distributions in Hyperons

Dilepton production using meson or hyperon beams offers a means of determining parton distributions of these unstable hadrons. Many important features of nucleon parton distributions, such as the flavor structure and the nature of the non-perturbative sea, find their counterparts in mesons and hyperons. Information about meson and hyperon parton structure could provide valuable new insight into nucleon parton distributions. Furthermore, certain aspects of the nucleon structure, such as the strange quark content of the nucleon, could be probed with kaon beams.

No data exist for hyperon-induced dilepton production. The observation of a large $\bar{d}/\bar{u}$ asymmetry in the proton has motivated Alberg et al. [132, 133] to consider the sea-quark distributions in the Σ. The meson-cloud model implies a $\bar{d}/\bar{u}$ asymmetry in the Σ^+ even larger than that of the proton. However, the opposite effect is expected from SU(3) symmetry. Although relatively intense Σ^+ beams have been produced for recent experiments at Fermilab, this experiment appears to be very challenging because of large pion, kaon, and proton contaminations in the beam.

6. FUTURE PROSPECTS

6.1 $\bar{d}/\bar{u}$ at Large and Small x

The interplay between the perturbative and non-perturbative components of the nucleon sea remains to be better determined. Since the perturbative process gives a symmetric $\bar{d}/\bar{u}$ while the non-perturbative process is needed to generate an asymmetric $\bar{d}/\bar{u}$ sea, the relative importance of these two components is directly reflected in the $\bar{d}/\bar{u}$ ratios. Thus, it would be very important to extend the DY measurements to kinematic regimes beyond the current limits.

The new 120 GeV Fermilab Main Injector (FMI) and the proposed 50 GeV Japanese Hadron Facility [134] (JHF) present opportunities for extending the $\bar{d}/\bar{u}$ measurement to larger x ($x > 0.25$). For given values of x_1 and x_2, the DY cross section is proportional to $1/s$, where s is the square of the center-of-mass energy. Hence the DY cross section at 50 GeV is roughly 16 times greater than that at 800 GeV! Figure 15 shows the expected statistical accuracy for $\sigma(p+d)/2\sigma(p+p)$ at JHF [135] compared with the data from E866 and a proposed measurement [136] using the 120 GeV proton beam at the FMI. A definitive measurement of the $\bar{d}/\bar{u}$ over the region $0.25 < x < 0.7$ could indeed be obtained at FMI and JHF.

At the other end of the energy scale, RHIC will operate soon in the range $50 \leq \sqrt{s} \leq 500$ GeV/nucleon. The capability of accelerating and colliding a variety of beams from $p+p$, $p+A$, to $A+A$ at RHIC offers a unique opportunity to extend the DY $\bar{d}/\bar{u}$ measurement to very small x.

6.2 W Production

To disentangle the $\bar{d}/\bar{u}$ asymmetry from the possible CSV effect, one could consider W boson production, a generalized DY process, in $p+p$ collision at RHIC. An interesting quantity to be measured is the ratio of the $p+p \to W^+ + X$ and $p+p \to W^- + X$ cross sections [137]. It can be shown that this ratio is very sensitive to $\bar{d}/\bar{u}$. An important feature of the W production asymmetry in $p+p$ collision is that it is completely free from the assumption of charge symmetry. Figure 16 shows the predictions for $p+p$ collision at $\sqrt{s} = 500$ GeV. The dashed curve corresponds to the $\bar{d}/\bar{u}$ symmetric MRS S0$'$ [138] structure functions, while the solid and dotted curves are for the $\bar{d}/\bar{u}$ asymmetric structure function MRST and MRS(R2), respectively. Figure 16 clearly shows that W asymmetry measurements at RHIC could provide an independent determination of $\bar{d}/\bar{u}$.

6.3 Strange Sea in the Nucleon

As discussed earlier, an interesting consequence of the meson-cloud model is that the s and $\bar{s}$ distributions in the proton could have very different shapes, even though the net amount of strangeness in the proton vanishes. By comparing the ν and $\bar{\nu}$ induced charm production, the CCFR collaboration found no difference between the s and $\bar{s}$ distributions [126]. More precise future measurements would be very helpful. Dimuon production experiments using $K^{\pm}$ beams might provide an independent determination of the $s/\bar{s}$ ratio of the proton, provided that our current knowledge on valence-quark distributions in kaons is improved. As discussed in Section 5.1, ongoing measurements of F^p_{1s} via parity-violating electron-nucleon scattering should shed much light on the possible difference between s and $\bar{s}$ distributions.

6.4 Sea Quark Polarization

Polarized DY and $W^{\pm}$ productions in polarized $p+p$ collision are planned at RHIC [139] and they have great potential for providing qualitatively new information about antiquark polarization. At large x_F region ($x_F > 0.2$), the longitudinal spin asymmetry A_{LL} in the $p+p$ DY process is given by [140, 141]

$$A^{DY}_{LL}(x_1, x_2) \approx g_1(x_1)/F_1(x_1) \times \frac{\Delta\bar{u}}{\bar{u}}(x_2), \tag{33}$$

where $g_1(x)$ is the proton polarized structure function measured in DIS, and $\Delta\bar{u}(x)$ is the polarized $\bar{u}$ distribution function.

Eq. 33 shows that $\bar{u}$ polarization can be determined using polarized DY at RHIC. Additional information on the sea-quark polarization can be obtained via $W^{\pm}$ production [142]. The parity-violating nature of W production implies that only one of the two beams need to be polarized. At positive x_F (along the direction of the polarized beam), one finds[142],

$$A^{W^+}_L \approx \frac{\Delta u}{u}(x_2), \quad \text{and} \quad A^{W^-}_L \approx \frac{\Delta d}{d}(x_2), \tag{34}$$

where A^W_L is the single-spin asymmetry for W production. Eq. 34 shows that the flavor dependence of the sea-quark polarization can be revealed via $W^{\pm}$ production at RHIC.

7. CONCLUSION

The flavor asymmetry of the nucleon sea has been clearly established by recent DIS and DY experiments. The surprisingly large asymmetry between $\bar{u}$ and $\bar{d}$, completely unexplained by perturbative QCD, strongly supports the view that virtual meson-baryon components play an important role in describing the parton distributions of the nucleon. The flavor and spin structures of the nucleon are shown to be closely connected in the virtual meson-baryon models. Future experiments will test and refine these models. They will further illuminate the interplay between the perturbative and non-perturbative nature of the nucleon sea.

Acknowledgment

We are grateful to our collaborators on the Fermilab E772 and E866. This work was supported by the US Department of Energy, Nuclear Science Division, under contract W-7405-ENG-36.

References

[1] E. D. Bloom et al., Phys. Rev. Lett. **23** (1969) 930.

[2] M. Breidenbach et al., Phys. Rev. Lett. **23** (1969) 935.

[3] R. P. Feynman, Photon-Hadron Interactions (Benjamin, New York, 1972).

[4] K. F. Liu et al., Phys. Rev. **D59** (1999) 112001.

[5] J. D. Bjorken, Phys. Rev. **179** (1969) 1547.

[6] R. P. Feynman, Phys. Rev. Lett. **23** (1969) 1415.

[7] S. D. Drell, D. J. Levy and T. M. Yan, Phys. Rev. **187** (1969) 2159.

[8] S. D. Drell, D. J. Levy and T. M. Yan, Phys. Rev. **D1** (1970) 1035; **D1** (1970) 1617.

[9] N. G. Cabbibo, G. Parisi, M. Testa and A. Verganelakis, Lett. Nuovo Cimento **4** (1970) 569.

[10] T. D. Lee and S. D. Drell, Phys. Rev. **D5** (1972) 1738.

[11] J. D. Bjorken and E. A. Paschos, Phys. Rev. **185** (1969) 1975.

[12] J. Kuti and V. F. Weisskopf, Phys. Rev. **D4** (1971) 3418.

[13] P. V. Landschoff and J. C. Polkinghorne, Nucl. Phys. **B28** (1971) 240.

[14] M. Gell-Mann, Phys. Lett. **8** (1964) 214.

[15] G. Zweig, CERN Preprint 8182/TH401, 8419/TH412 (1964).

[16] J. I. Friedman and H. W. Kendall, Annu. Rev. Nucl. Sci. **22** (1972) 203.

[17] J. G. H. de Groot et al., Z. Phys. **C1** (1979) 143.

[18] H. Abromowicz et al., Z. Phys. **C15** (1982) 19.

[19] J. M. Conrad, M. H. Shaevitz and T. Bolton, Rev. Mod. Phys. **70** (1998) 1341.

[20] K. Gottfried, Phys. Rev. Lett. **18** (1967) 1174.

[21] J. D. Bjorken, Proc. 1967 Int. Sym. on Electron and Photon Interactions at High Energies, Stanford, CA (1967) 109.

[22] E. D. Bloom et al., Proc. 15th Int. Conf. on High Energy Phys., Kiev, USSR (1970).

[23] E. D. Bloom, Proc. 6th Int. Sym. on Electron and Photon Interactions at High Energies, edited by H. Rollnik and W. Pfeil (North-Hollan, Amsterdam, 1974) 227.

[24] R. D. Field and R. P. Feynman, Phys. Rev. **D15** (1977) 2590.

[25] Y. Watenabe et al., Phys. Rev. Lett. **35** (1975) 898.

[26] C. Chang et al., Phys. Rev. Lett. **35** (1975) 901.

[27] B. A. Gordon et al., Phys. Rev. **D20** (1979) 2645.

[28] J. J. Aubert et al., Nucl. Phys. **B293** (1987) 740.

[29] A. C. Benvenuti et al., Phys. Lett. **B237** (1990) 599.

[30] A. Bodek et al., Phys. Rev. **D20** (1979) 1471.

[31] D. W. Duke and J. F. Owens, Phys. Rev. **D30** (1984) 49.

[32] E. Eichten, I. Hinchliffe, K. Lane and C. Quigg, Rev. Mod. Phys. **56** (1984) 579; Rev. Mod. Phys. **58** (1985) 1065.

[33] M. Diemoz, F. Ferroni, E. Longo and G. Martinelli, Z. Phys. **C39** (1988) 21.

[34] A. D. Martin, R. G. Roberts and W. J. Stirling, Phys. Lett. **B206** (1988) 327.

[35] P. Aurenche et al., Phys. Rev. **D39** (1989) 3275.

[36] J. H. Christensen et al., Phys. Rev. Lett. **25** (1970) 1523.

[37] S. D. Drell and T. M. Yan, Phys. Rev. Lett. **25** (1970) 316.

[38] S. W. Herb et al., Phys. Rev. Lett. **39** (1977) 252.

[39] D. M. Kaplan et al., Phys. Rev. Lett. **40** (1977) 435.

[40] A. S. Ito et al., Phys. Rev. **D23** (1981) 604.

[41] S. R. Smith et al., Phys. Rev. Lett. **46** (1981) 1607.

[42] J. J. Aubert et al., Phys. Lett. **B123** (1983) 295.

[43] J. Ashman et al., Phys. Lett. **B202** (1988) 603.

[44] D. Allasia et al., Phys. Lett. **B249** (1990) 366.

[45] P. Amaudruz et al., Nucl. Phys. **B441** (1995) 3.

[46] P. Amaudruz et al., Phys. Rev. Lett. **66** (1991) 2712.

[47] L. W. Whitlow et al., Phys. Lett. **B282** (1992) 475.

[48] A. C. Benvenuti et al., Phys. Lett. **B237** (1990) 592.

[49] M. Arneodo et al., Nucl. Phys. **B333** (1990) 1.

[50] M. Arneodo et al., Phys. Rev. **D50** (1994) R1.

[51] P. Amaudruz et al., Phys. Lett. **B295** (1992) 159.

[52] M. Arneodo et al., Nucl. Phys. **B487** (1997) 3.

[53] M. Arneodo et el., Phys. Lett. **B364** (1995) 107.

[54] M. Arneodo et al., Nucl. Phys. **B483** (1997) 3.

[55] D. F. Geesaman, K. Saito and A. W. Thomas, Annu. Rev. Nucl. Part. Sci. **45** (1995) 337.

[56] C. H. Llewllyn-Smith, Phys. Lett. **B128** (1983) 107; M. Ericson and A. W. Thomas, Phys. Lett. **B128** (1983) 112; E. L. Berger, F. Coester and R. B. Wiringa, Phys. Rev. **D29** (1984) 398.

[57] D. M. Alde et al., Phys. Rev. Lett. **64** (1990) 2479.

[58] F. E. Close, R. L. Jaffe, R. G. Roberts and G. G. Ross, Phys. Rev. **D31** (1985) 1004.

[59] P. L. McGaughey et al., Phys. Rev. Lett. **69** (1991) 1726.

[60] S. D. Ellis and W. J. Stirling, Phys. Lett. **B256** (1991) 258.

[61] E. Eichten, I. Hinchliffe and C. Quigg, Phys. Rev. **D45** (1992) 2269.

[62] A. D. Martin, R. G. Roberts, W. J. Stirling and R. S. Thorne, Eur. Phys. J. **C4** (1998) 463.

[63] S. Kumano, Phys. Lett. **B342** (1995) 339.

[64] A. Baldit et al., Phys. Lett. **B332** (1994) 244.

[65] E. A. Hawker et al., Phys. Rev. Lett. **80** (1998) 3715.

[66] R. S. Towell et al., to be published (1999).

[67] H. L. Lai et al., Phys. Rev. **D55** (1997) 1280.

[68] A. D. Martin, R. G. Roberts and W. J. Stirling, Phys. Lett. **B387** (1996) 419.

[69] J. C. Peng et al., Phys. Rev. **D58** (1998) 092004.

[70] M. Gronau, F. Ravndal and Y. Zarmi, Nucl. Phys. **B51** (1973) 611.

[71] J. Ashman et al., Z. Phys. **C52** (1991) 361.

[72] D. Allasia et al., Phys. Lett. **B135** (1984) 231.

[73] H. Abramowicz et al., Z. Phys. **C25** (1984) 29.

[74] J. Levelt, P. J. Mulders and A. W. Schreiber, Phys. Lett. **B263** (1991) 498.

[75] K. Ackerstaff et al., Phys. Rev. Lett. **81** (1998) 5519.

[76] M. Glück, E. Reya and A. Vogt, Z. Phys. **C67** (1995) 433.

[77] L. L. Frankfurt et al., Phys. Lett. **B230** (1989) 141.

[78] F. E. Close and R. G. Milner, Phys. Rev. **D44** (1991) 3691.

[79] B. Adeva et al., Phys. Lett. **B369** (1997) 93; B. Adeva et al., Phys. Lett. **420** (1998) 180.

[80] K. Akerstaff et al., hep-ex/9906035 (1999).

[81] M. Glück, E. Reya and A. Vogt, Eur. Phys. J. **C5** (1998) 461.

[82] H. L. Lai et al., hep-ph/9903282, to be published in Eur. Phys. J. (1999).

[83] H. L. Lai, private communication (1999).

[84] F. Abe et al., Phys. Rev. Lett. **81** (1998) 5754.

[85] R. D. Ball et al., Phys. Lett. **B329** (1994) 505.

[86] D. A. Ross and C. T. Sachrajda, Nucl. Phys. **B149** (1979) 497.

[87] F. M. Steffens and A. W. Thomas, Phys. Rev. **C55** (1997) 900.

[88] A. W. Thomas, Phys. Lett. **B126** (1983) 97.

[89] J. D. Sullivan, Phys. Rev. **D5** (1972) 1732.

[90] S. Kumano, Phys. Rep. **303** (1998) 183.

[91] J. P. Speth and A. W. Thomas, Adv. Nucl. Phys. **24** (1998) 83.

[92] E. M. Henley and G. A. Miller, Phys. Lett. **251** (1990) 453.

[93] S. Kumano, Phys. Rev. **D43** (1991) 3067; **D43** (1991) 59; S. Kumano and J. T. Londergan, Phys. Rev. **D44** (1991) 717.

[94] A. Signal, A. W. Schreiber, and A. W. Thomas, Mod. Phys. Lett. **A6** (1991) 271.

[95] W. P. Hwang, J. Speth and G. E. Brown, Z. Phys. **A339** (1991) 383.

[96] A. Szczurek, J. Speth and G. T. Garvey, Nucl. Phys. **A570** (1994) 765.

[97] W. Koepf, L. L. Frankfurt and M. Strikman, Phys. Rev. **D53** (1996) 2586.

[98] W. Melnitchouk, J. Speth and A. W. Thomas, Phys. Rev. **D59** (1999) 014033.

[99] H. Holtzman, A. Szczurek and J. Speth, Nucl. Phys. **A596** (1996) 631.

[100] N. N. Nikolaev, W. Schaefer, A. Szczurek and J. Speth, Phys. Rev. **D60** (1999) 014004.

[101] T. P. Cheng and L. F. Li, Phys. Rev. Lett. **74** (1995) 2872.

[102] T. P. Cheng and L. F. Li, Phys. Lett. **B366** (1996) 365.

[103] K. Suzuki and W. Weise, Nucl. Phys. **A634** (1998) 141.

[104] A. Manohar and H. Georgi, Nucl. Phys. **B234** (1984) 189.

[105] A. Szczurek, A. Buchmans and A. Faessler, J. Phys. **C22** (1996) 1741.

[106] A. A. Belavin et al., Phys. Lett. **B59** (1975) 85.

[107] G. t'Hooft, Phys. Rev. Lett. **37** (1976) 8.

[108] T. Schaefer and E. Shuryak, Rev. Mod. Phys. **70** (1998) 323.

[109] A. E. Dorokhov and N. I. Kochelev, Phys. Lett. **B259** (1991) 335; **B335** (1993) 167.

[110] G. A. Miller, B. M. K. Nefkens and I. Slaus, Phys. Rep. **194** (1990) 1.

[111] E. M. Henley and G. A. Miller, *Mesons in Nuclei*, ed. M. Rho, D. H. Wilkinson. Amsterdam: North-Holland (1979).

[112] B. Ma, Phys. Lett. **B274** (1992) 111.

[113] B. Ma B, A. Schäfer and W. Greiner, Phys. Rev. **D47** (1993) 51.

[114] E. Sather, Phys. Lett. **B274** (1992) 433.

[115] J. T. Londergan et al., Phys. Lett. **B340** (1994) 115.

[116] E. N. Rodionov, A. W. Thomas and J. T. Londergan, Int. J. Mod. Phys. Lett. **A9** (1994) 1799.

[117] C. J. Benesh and T. Goldman, Phys. Rev. **C55** (1997) 441.

[118] C. J. Benesh and J. T. Londergan, Phys. Rev. **C58** (1998) 1218.

[119] J. T. Londergan and A. W. Thomas, *Progress in Particle and Nuclear Physics*, **41** (1998) 49.

[120] C. Boros, J. T. Londergan and A. W. Thomas, Phys. Rev. Lett. **81** (1998) 4075; Phys. Rev. **D59** (1999) 074021.

[121] A. Bodek et al., hep-ex/9904022 (1999).

[122] A. I. Signal and A. W. Thomas, Phys. Lett. **B191** (1987) 205.

[123] M. Burkardt and B. J. Warr, Phys. Rev. **D45** (1992) 958.

[124] X. D. Ji and J. Tang, Phys. Lett. **B362** (1995) 182.

[125] S. Brodsky and B-Q. Ma, Phys. Lett. **B381** (1996) 317.

[126] A. O. Bazarko et al., Z. Phys. **C65** (1995) 189.

[127] D. Kaplan and A. Manohar, Nucl. Phys. **B310** (1988) 527.

[128] G. Garvey, W. Louis and H. White, Phys. Rev. **C48** (1993) 761.

[129] B. Mueller et al., Phys. Rev. Lett. **78** (1997) 3824.

[130] K. Aniol et al., Phys. Rev. Lett. **82** (1999) 1096.

[131] A. W. Schreiber and A. W. Thomas, Phys. Lett. **B215** (1998) 141.

[132] M. Alberg et al., Phys. Lett. **B389** (1996) 367.

[133] M. Alberg, T. Falter and E. M. Henley, Nucl. Phys. **A644** (1998) 93.

[134] JHF Project Office. *Proposal for Japan Hadron Facility*, KEK Rep. **97-3** (1997).

[135] C. N. Brown, unpublished (1998).

[136] D. Geesaman et al., *Fermilab proposal P906* (1999).

[137] J. C. Peng and D. M. Jansen, Phys. Lett. B **354** (1995) 460.

[138] A. D. Martin, W. J. Stirling and R. G. Roberts, Phys. Lett. B **306** (1993) 145.

[139] G. Bunce et al. Part. World **3** (1992) 1.

[140] J. M. Moss, *Int. Conf. Polarization Phenomena in Nucl. Phys., AIP Conf. Proc.* **339** (1994) 721.

[141] P. L. McGaughey, J. M. Moss and J. C. Peng, hep-ph/9905409, to be published in Annu. Rev. Nucl. Part. Sci. (1999).

[142] C. Bourrely and J. Soffer Phys. Lett. **B314** (1993) 132.

Table 1: Values of the integral $\int_0^1 (\bar{d}(x) - \bar{u}(x))dx$ for various parton distribution functions.

PDF	integral
CTEQ4M	0.108
MRS(R2)	0.162
GRV94	0.163
CTEQ5M	0.124
MRST	0.102
GRV98	0.126

Table 2: Comparison between the 450 GeV/c NA51 result and the 800 GeV/c E866 data point near $x_2 = 0.18$.

	$\langle x_2 \rangle$	$\langle x_F \rangle$	$\langle M_{\mu\mu} \rangle$(GeV)	$\sigma^{pd}/2\sigma^{pp}$	$\bar{d}/\bar{u}$
NA51	0.18	0.0	5.2	1.099 ± 0.039	1.96 ± 0.246
E866	0.182	0.192	9.9	1.091 ± 0.044	1.41 ± 0.146

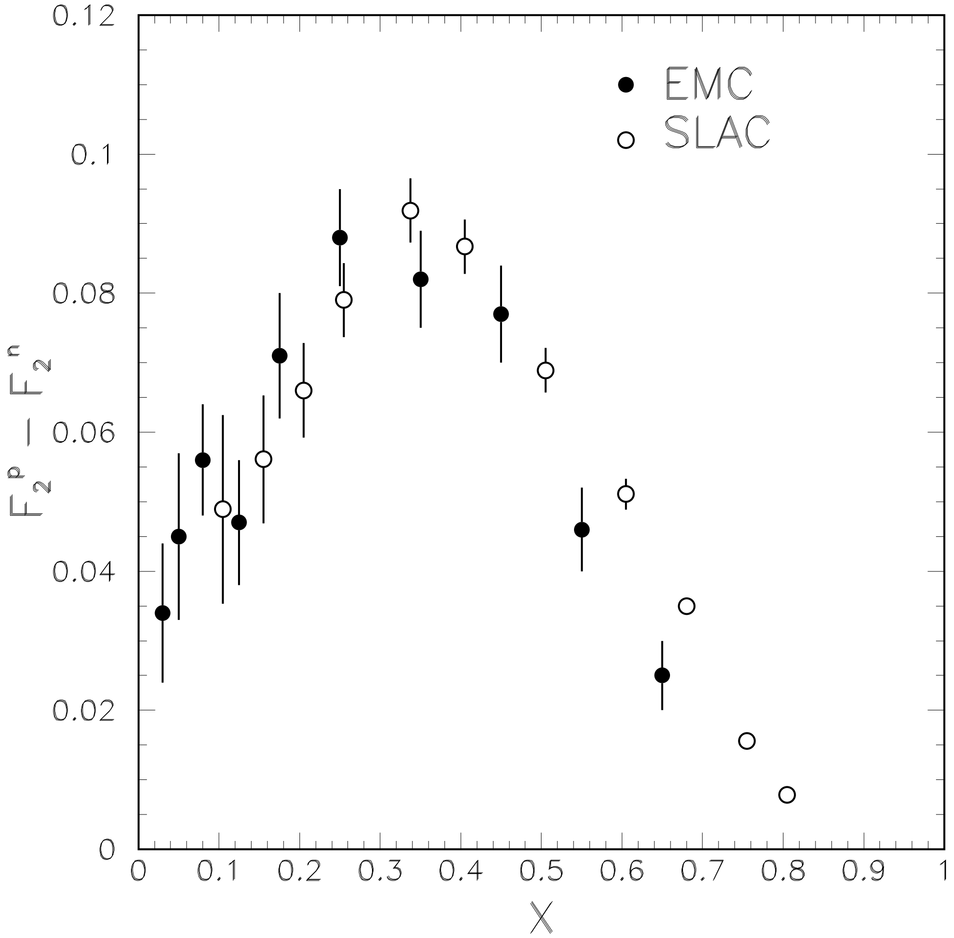

Figure 1: EMC [28] and SLAC [30] measurements of $F_2^p - F_2^n$.

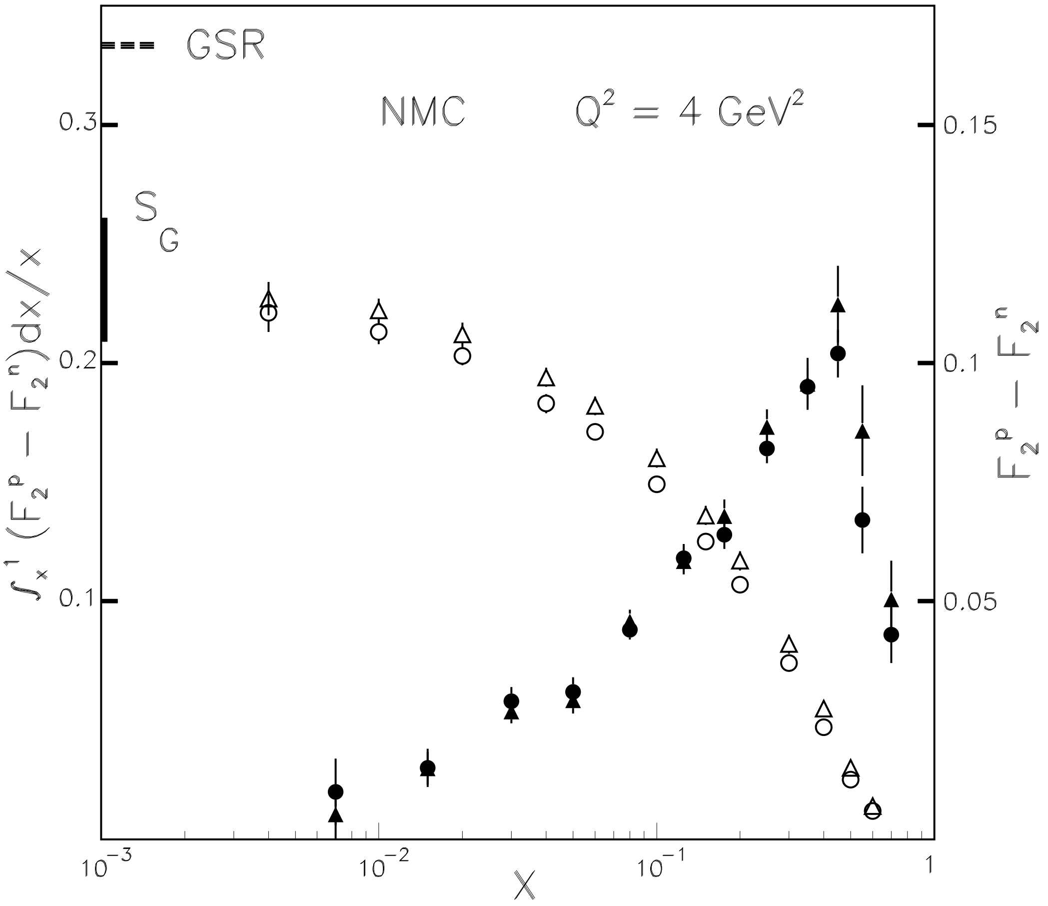

Figure 2: NMC measurements of $F_2^p - F_2^n$ (solid data points) and the Gottfried integral (open data points). The triangular data points correspond to results published in 1991 [46], while the circular data points represent a more recent analysis in 1994 [50]. The extrapolated value of Gottfried integral (S_G) and the expected GSR value are also indicated.

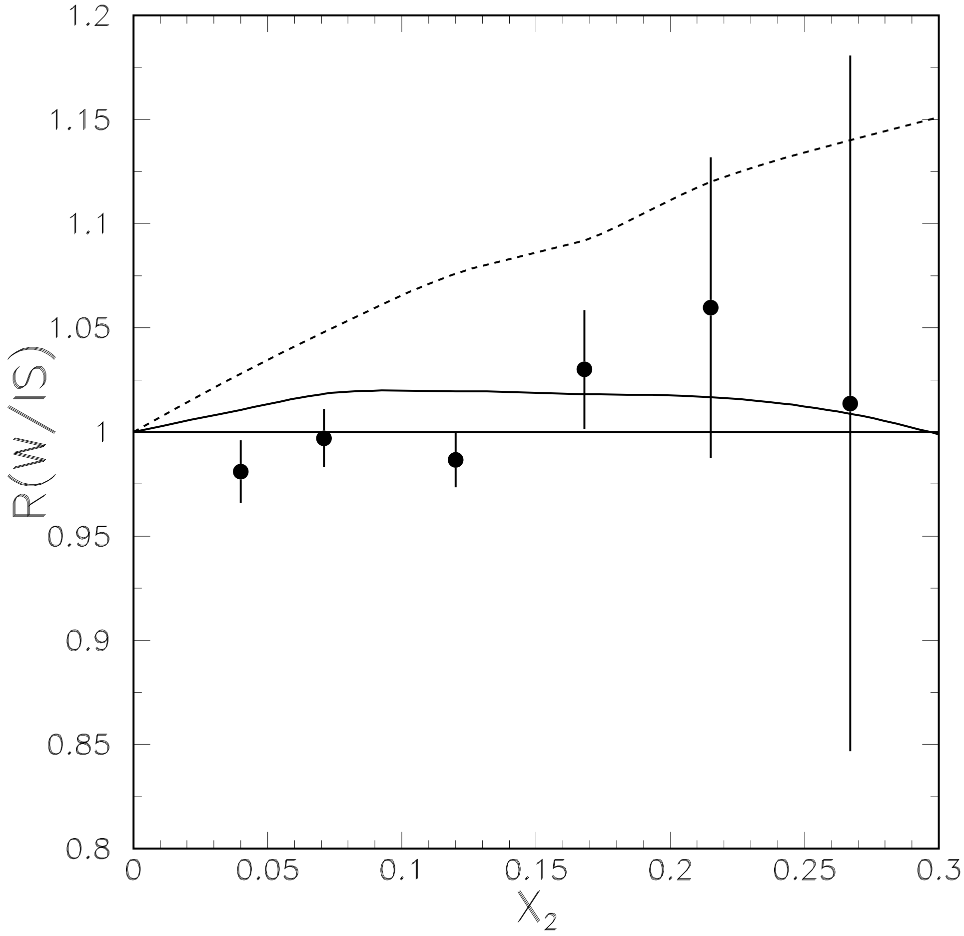

Figure 3: The ratios of W over isoscalar targets DY cross sections from E772 [59]. The dashed curve is a calculation using the $\bar{d}/\bar{u}$ asymmetric parton distributions suggested in Ref. [60]. The solid curve corresponds to a calculation using the recent MRST distribution functions.

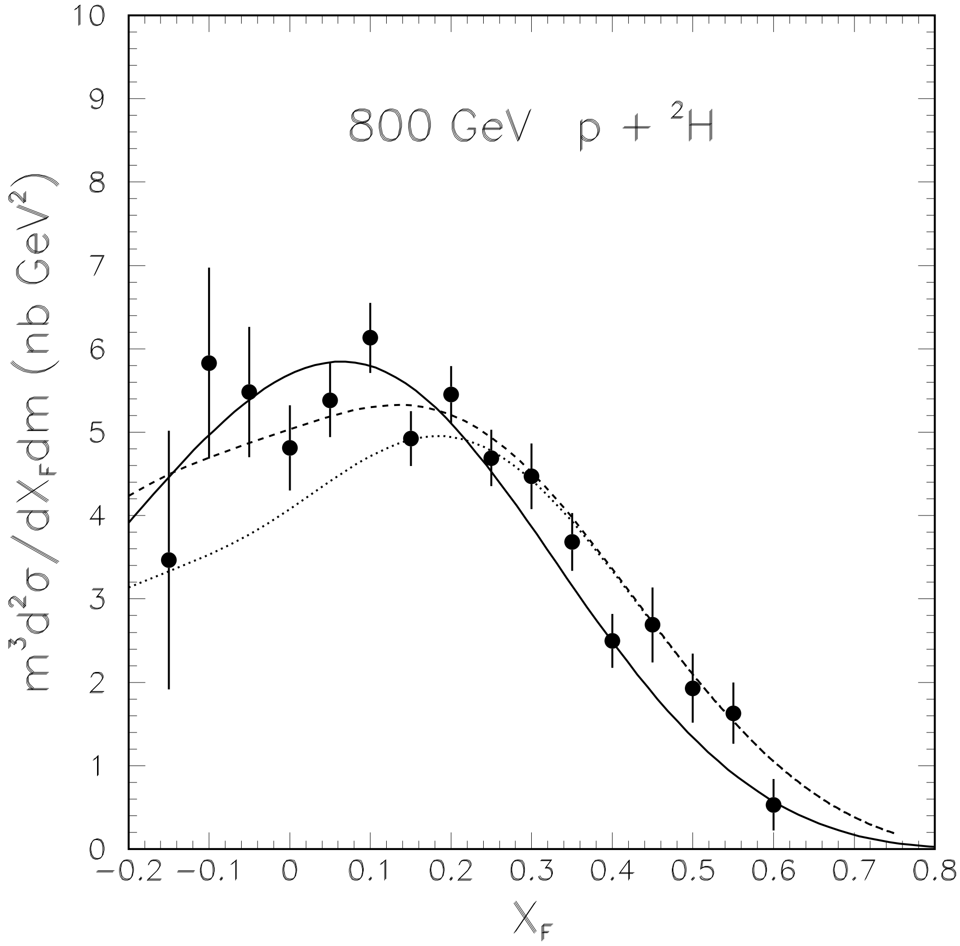

Figure 4: The $p+^2H$ DY differential cross sections from E772 [59]. The dotted (dashed) curve is a calculation using the parton distributions from Ref. [60] with (without) $\bar{d}/\bar{u}$ asymmetry. The solid curve uses the MRST distribution functions. These are leading-order calculations normalized to the data.

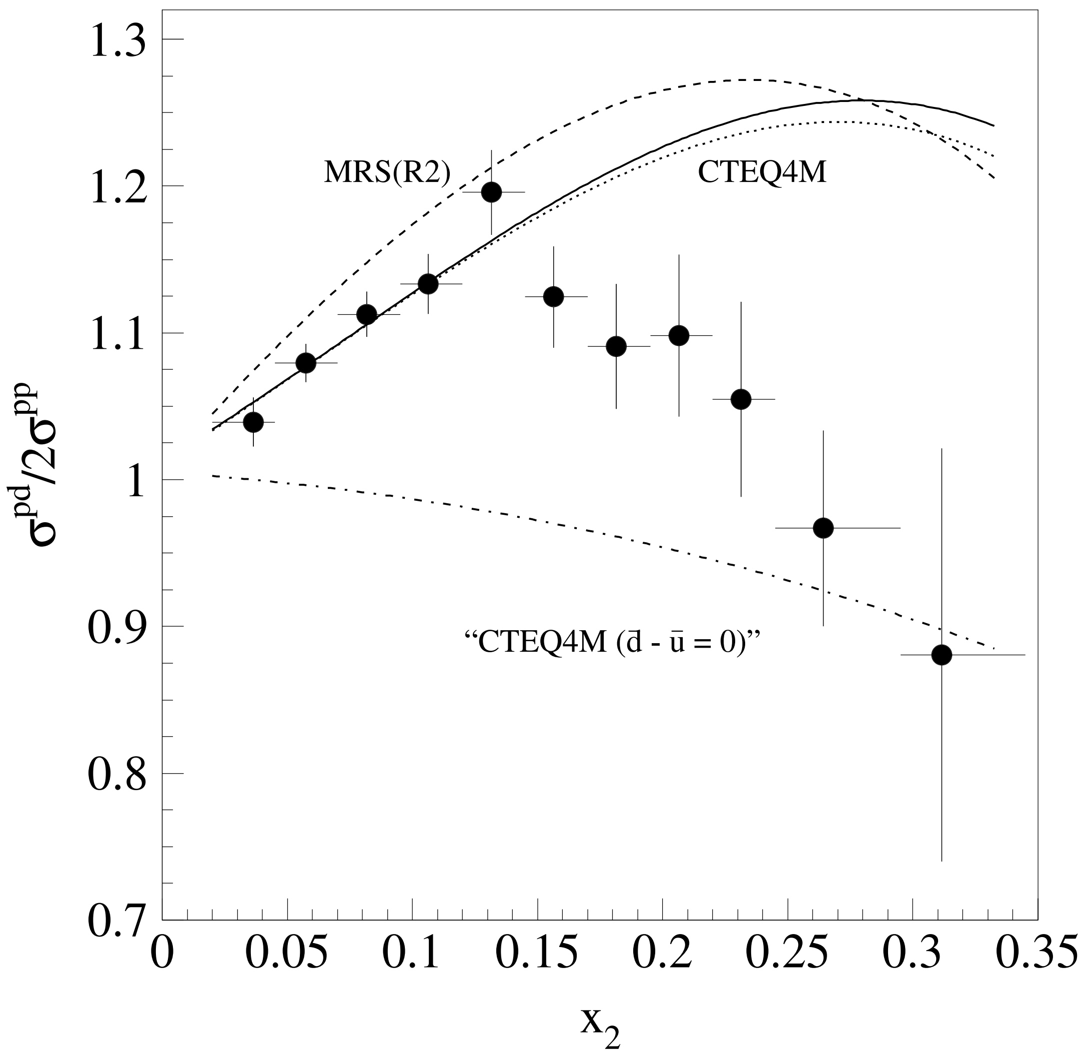

Figure 5: The ratio $\sigma^{pd}/2\sigma^{pp}$ of Drell-Yan cross sections *vs.* x_2. The curves are next-to-leading order calculations, weighted by acceptance, of the Drell-Yan cross section ratio using the CTEQ4M and MRS(R2) parton distributions. Also shown is a leading-order calculation using CTEQ4M (dotted). In the lower CTEQ4M curve $\bar{d}-\bar{u}$ has been arbitrarily set to 0 as described in the text. The errors are statistical only. There is an additional 1% systematic uncertainty common to all points.

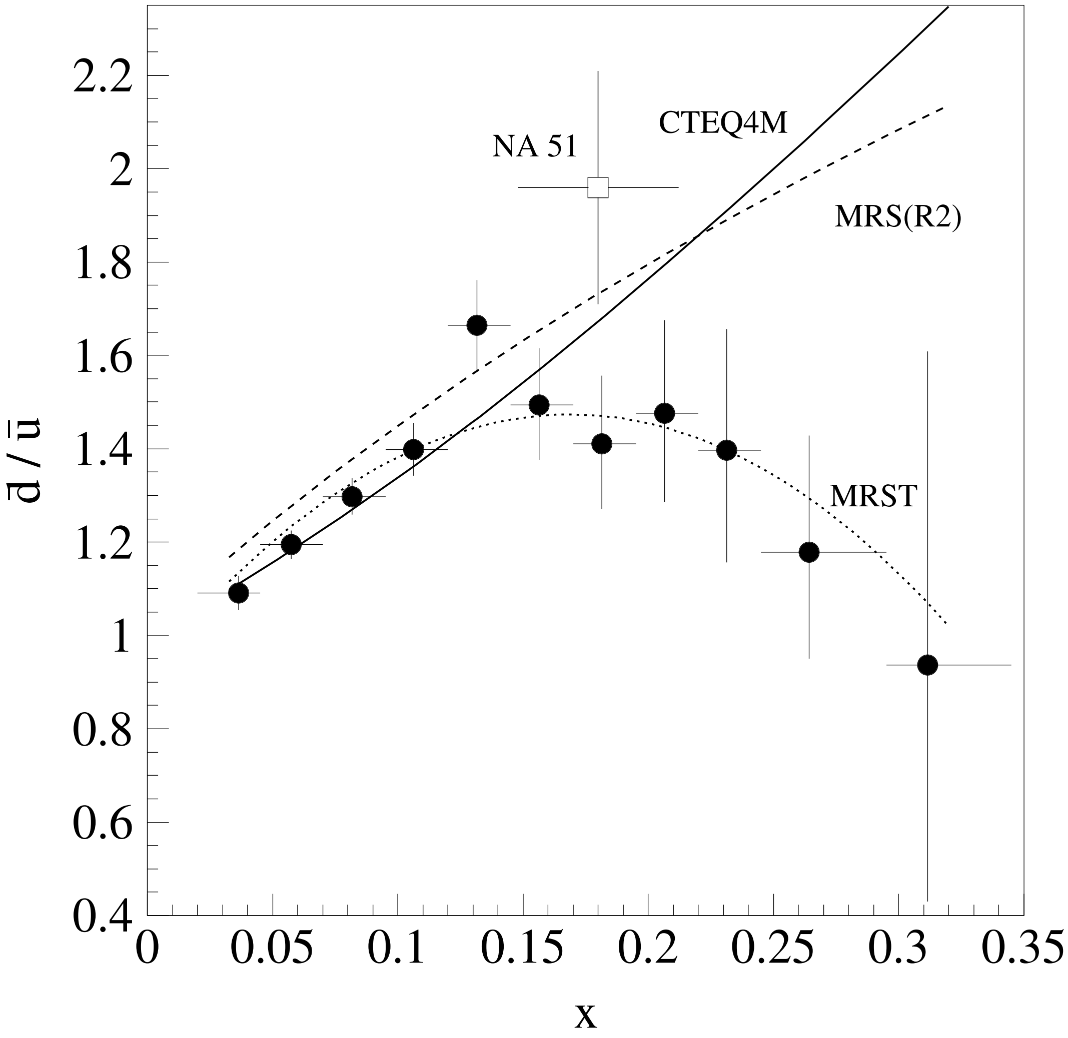

Figure 6: The ratio of $\bar{d}/\bar{u}$ in the proton as a function of x_2 extracted from the Fermilab E866 cross section ratio. The curves are from various parton distributions. The error bars indicate statistical errors only. An additional systematic uncertainty of ± 0.032 is not shown. Also shown is the result from NA51, plotted as an open box.

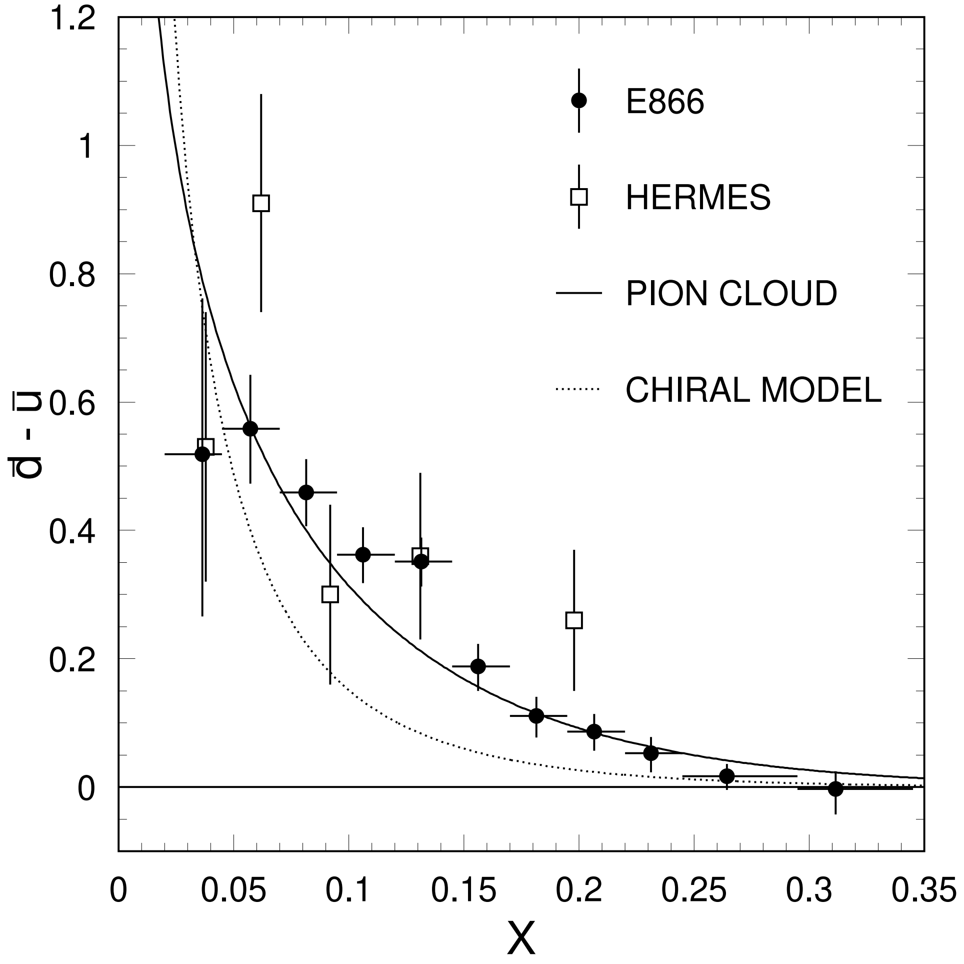

Figure 7: Comparison of the E866 [65] $\bar{d}-\bar{u}$ results at $Q^2 = 54$ GeV^2/c^2 with the predictions of pion-cloud and chiral models as described in the text. The data from HERMES [75] are also shown.

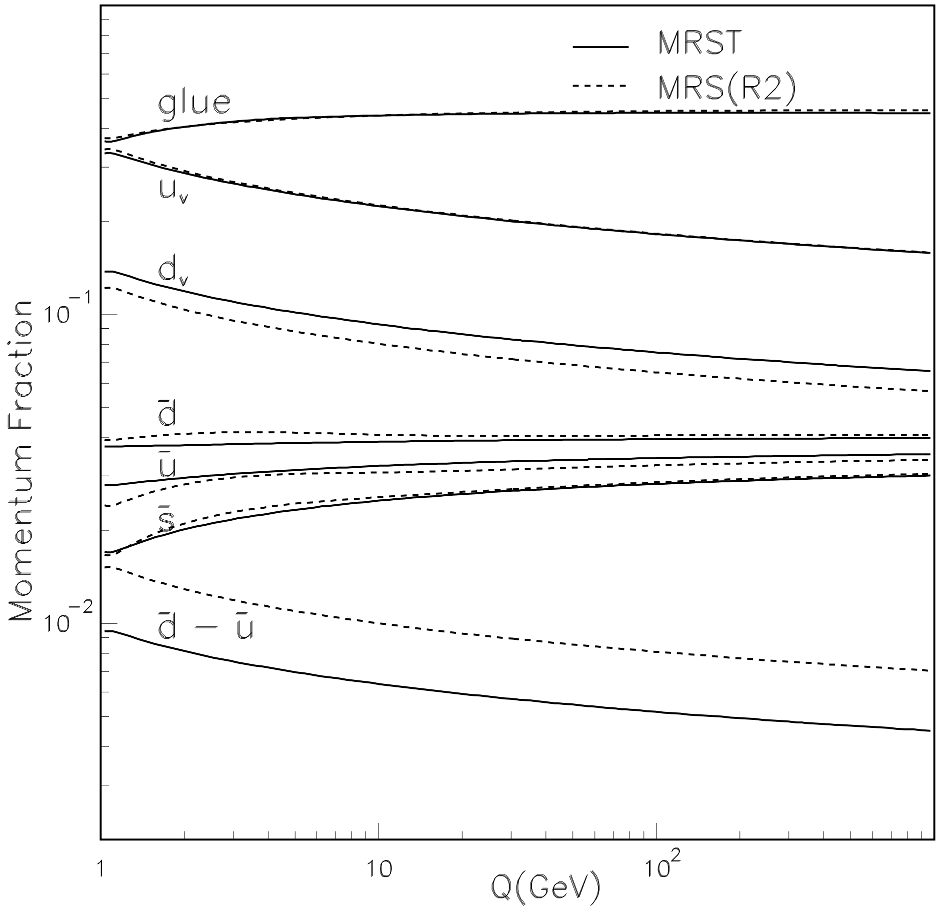

Figure 8: Q-dependence of the proton's momentum carried by various partons calculated using the MRS(R2) and MRST parton distribution functions.

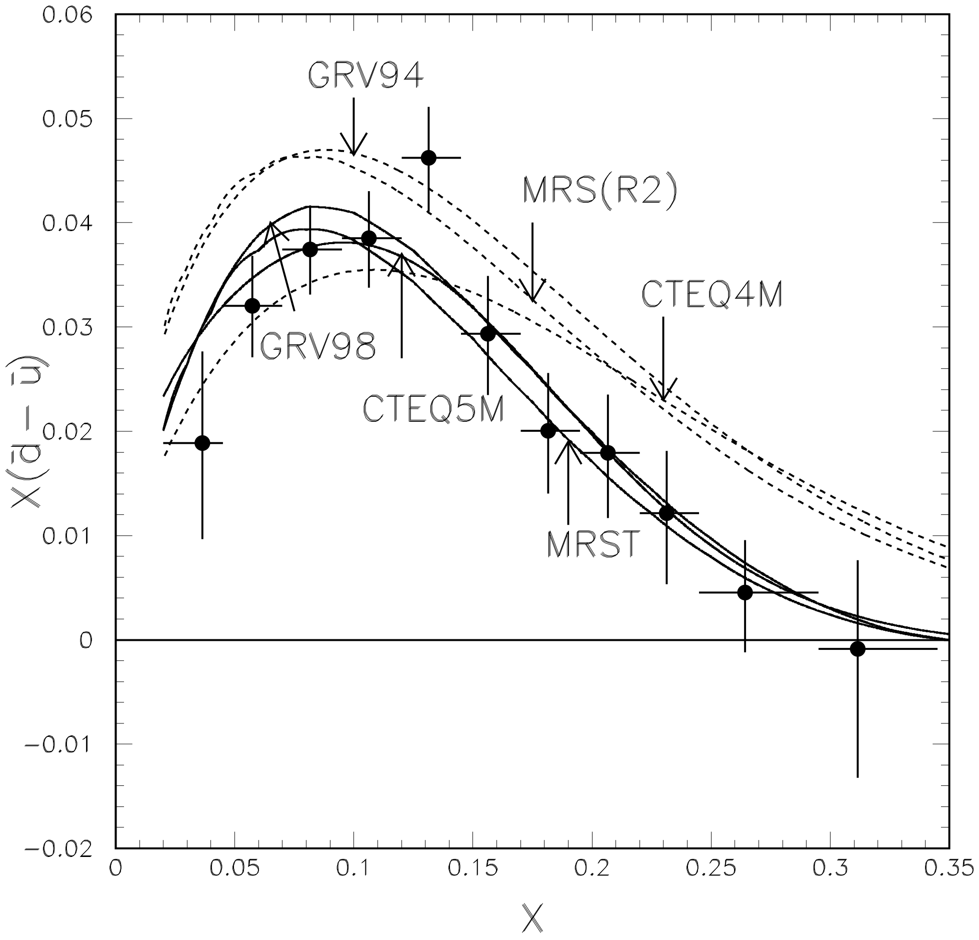

Figure 9: Comparison between the $x(\bar{d} - \bar{u})$ results from E866 with the parametrizations of various parton distribution functions. The dashed (solid) curves correspond to PDFs before (after) the E866 results were obtained.

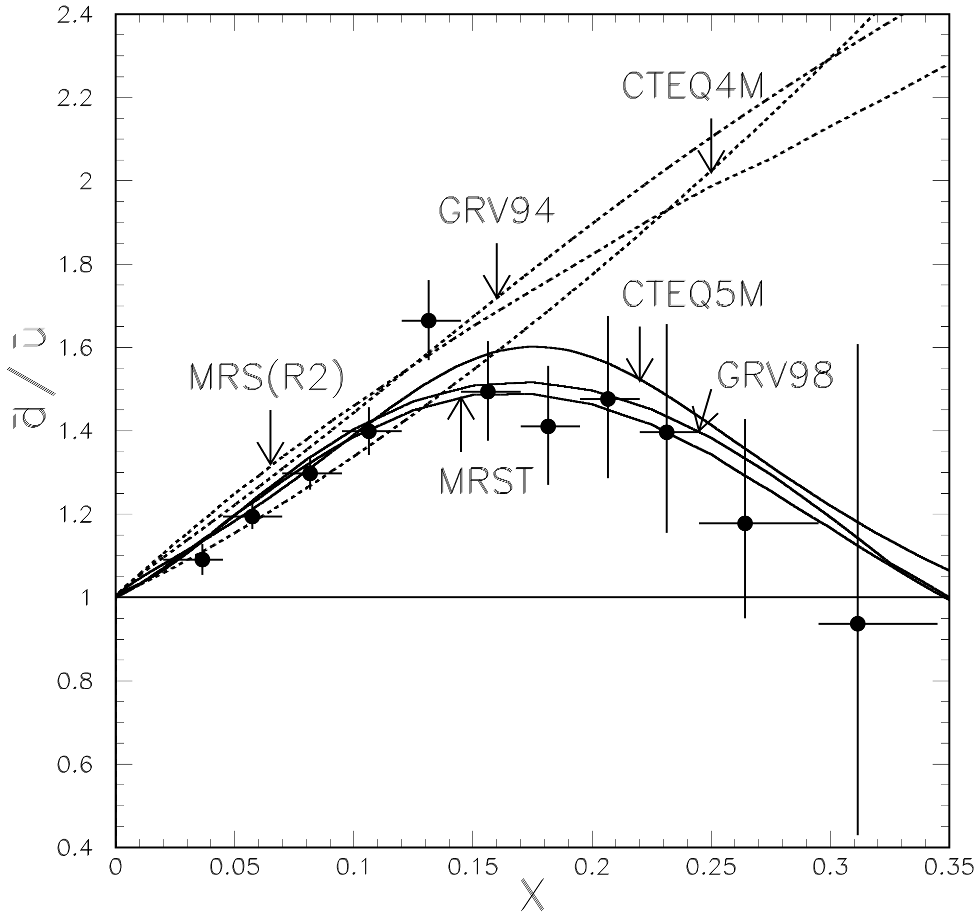

Figure 10: Comparison between the $\bar{d}/\bar{u}$ results from E866 with the parametrizations of various parton distribution functions. The dashed (solid) curves correspond to PDFs before (after) the E866 results were obtained.

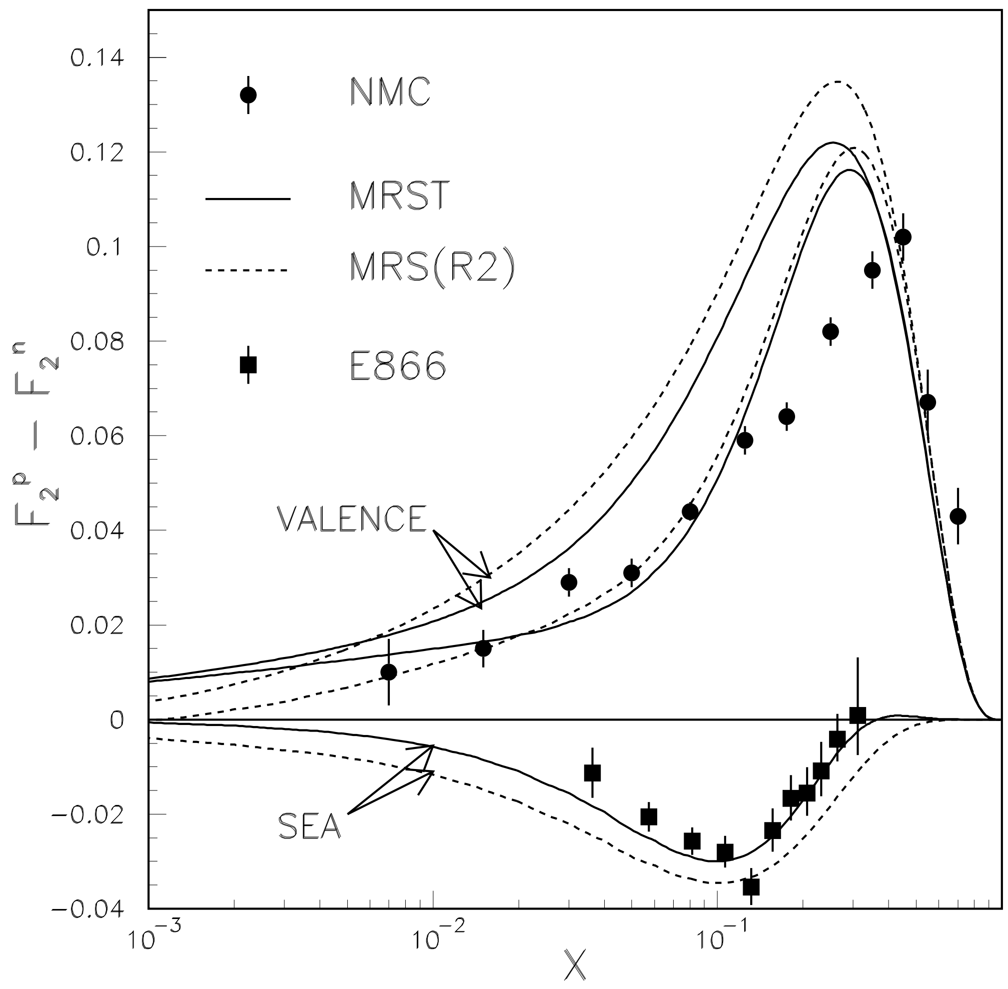

Figure 11: $F_2^p - F_2^n$ as measured by NMC at $Q^2 = 4$ GeV^2 compared with predictions based on the MRS(R2) and MRST parametrizations. Also shown are the E866 results, evolved to $Q^2 = 4$ GeV^2, for the sea-quark contribution to $F_2^p - F_2^n$. For each prediction, the top (bottom) curve is the valence (sea) contribution and the middle curve is the sum of the two.

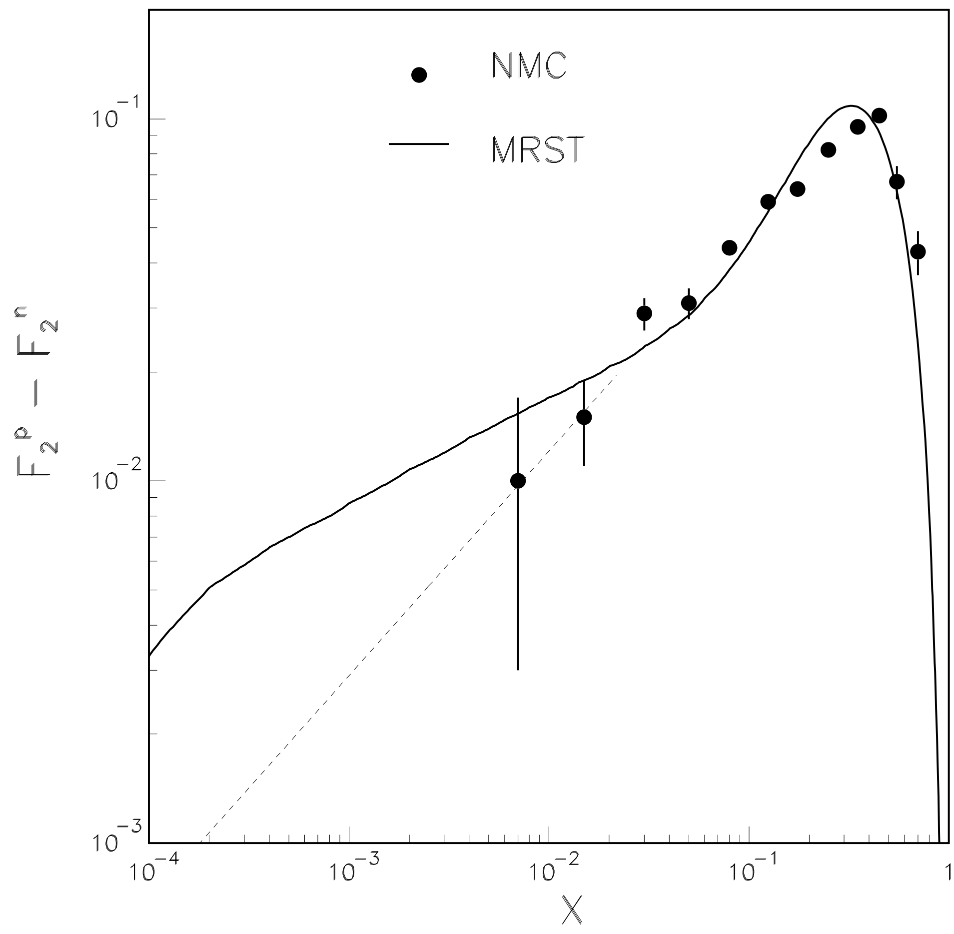

Figure 12: $F_2^p - F_2^n$ as measured by NMC at $Q^2 = 4$ GeV^2 compared with parametrization of MRST. The dashed curve corresponds to $0.21x^{0.62}$, a parametrization assumed by the NMC for the unmeasured small-x region when the Gottfried integral was evaluated.

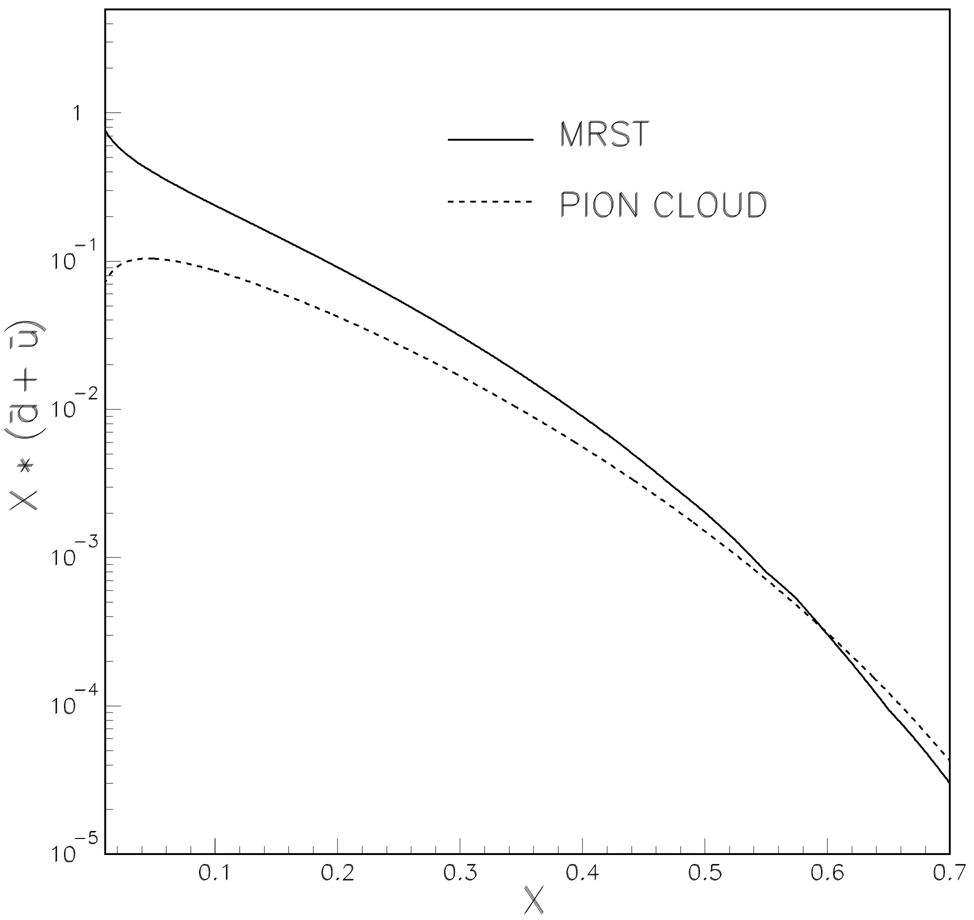

Figure 13: Comaprison of $x(\bar{d}+\bar{u})$ obtained from the valence quarks in the pion cloud with the parametrization of the MRST parton distribution functions.

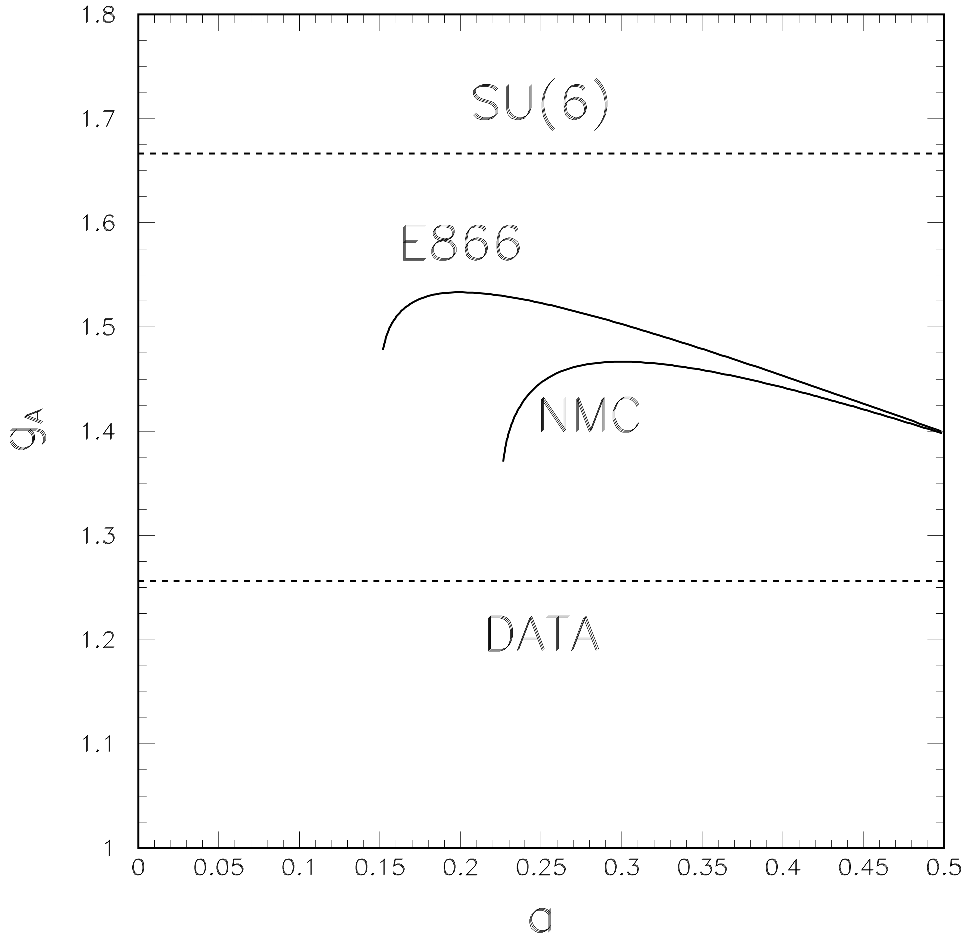

Figure 14: g_A as a function of a determined from Eqs. 21 and 30. The upper and lower solid curve is obtained by using the values $\bar{d}-\bar{u}$ determined by E866 and NMC, respectively. The values of g_A for the SU(6) limit and from the experiments are also indicated by the dashed curves.

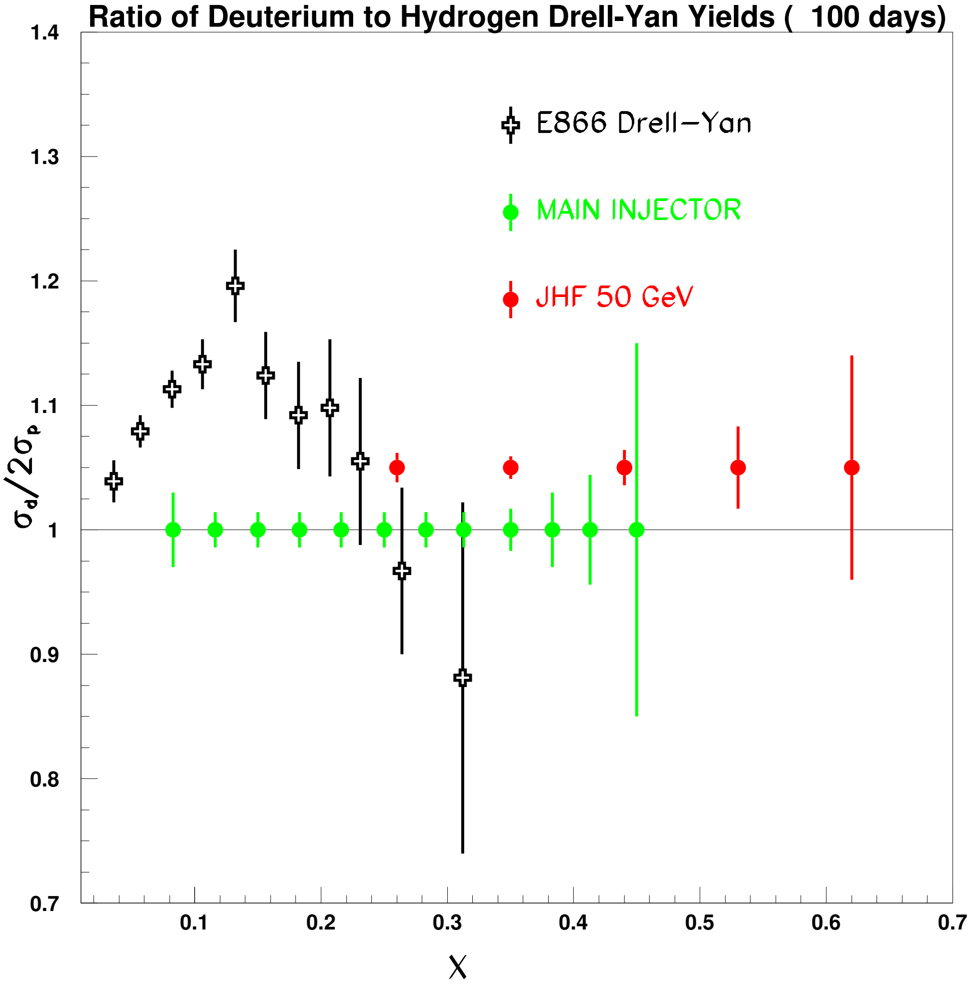

Figure 15: Projected statistical accuracy for $\sigma_d/2\sigma_p$ in a 100-day run at JHF. The E866 data and the projected sensitivity for a proposed measurement [136] at the 120 GeV Fermilab Main-Injector are also shown.

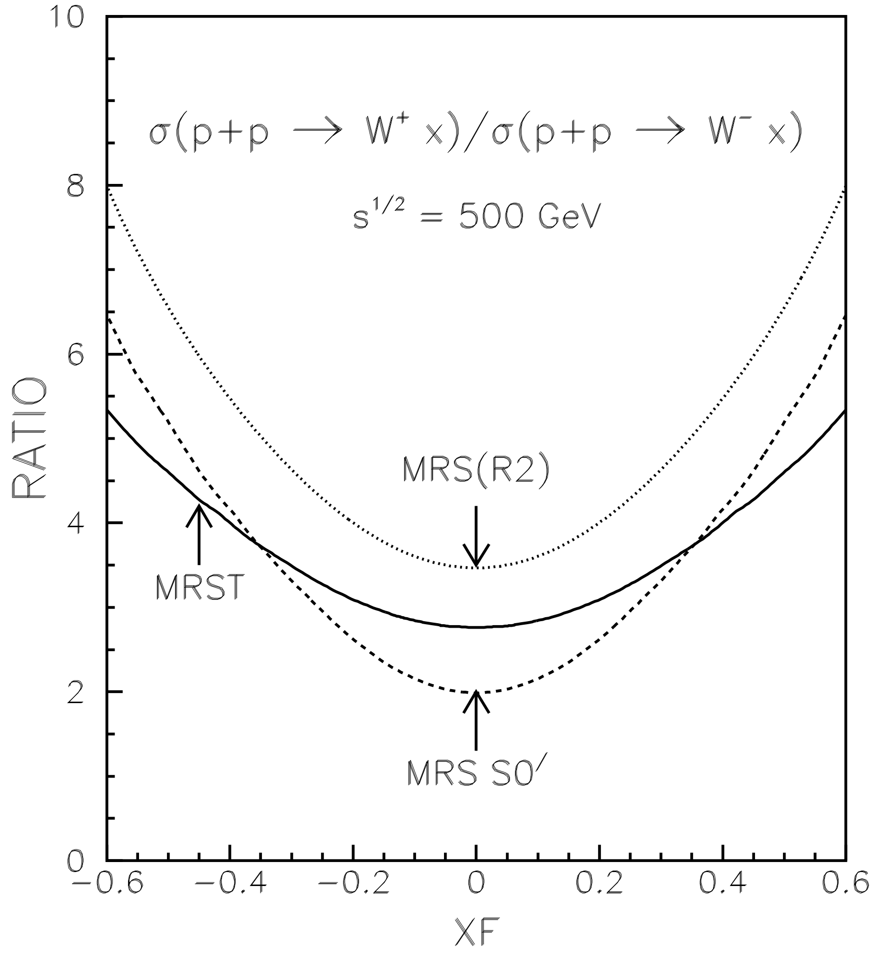

Figure 16: Predictions of $\sigma(p + p \to W^+X)/\sigma(p + p \to W^-X)$ as a function of x_F at $\sqrt{s} =$ 500 GeV. The dashed curve corresponds to the $\bar{d}/\bar{u}$ symmetric MRS S0$'$ structure functions, while the solid and dotted curves are for the $\bar{d}/\bar{u}$ asymmetric structure function MRST and MRS(R2), respectively.